Journal of Controlled Release 349 (2022) 143–155

Contents lists available at ScienceDirect

Journal of Controlled Release

journal homepage: www.elsevier.com/locate/jconrel

Review article

Tissue engineered drug delivery vehicles: Methods to monitor and regulate the release behavior

Carmen J. Gil [a], Lan Li [b], Boeun Hwang [a], Melissa Cadena [a], Andrea S. Theus [a], Tyler A. Finamore [b], Holly Bauser-Heaton [c,d,e], Morteza Mahmoudi [f], Ryan K. Roeder [b], Vahid Serpooshan [a,c,d,*]

[a] Department of Biomedical Engineering, Emory University School of Medicine and Georgia Institute of Technology, Atlanta, GA 30322, USA
[b] Bioengineering Graduate Program, Department of Aerospace and Mechanical Engineering, University of Notre Dame, Notre Dame, IN 46556, USA
[c] Department of Pediatrics, Emory University School of Medicine, Atlanta, GA 30322, USA
[d] Children's Healthcare of Atlanta, Atlanta, GA 30322, USA
[e] Sibley Heart Center at Children's Healthcare of Atlanta, Atlanta, GA 30322, USA
[f] Department of Radiology and Precision Health Program, Michigan State University, East Lansing, MI 48864, USA

ARTICLE INFO

Keywords:
Tissue engineering scaffolds
Drug delivery
Controlled release
Noninvasive imaging
Molecular contrast agents
Nanoparticles
Microparticles
Quantum dots

ABSTRACT

Tissue engineering is a rapidly evolving, multidisciplinary field that aims at generating or regenerating 3D functional tissues for *in vitro* disease modeling and drug screening applications or for *in vivo* therapies. A variety of advanced biological and engineering methods are increasingly being used to further enhance and customize the functionality of tissue engineered scaffolds. To this end, tunable drug delivery and release mechanisms are incorporated into tissue engineering modalities to promote different therapeutic processes, thus, addressing challenges faced in the clinical applications. In this review, we elaborate the mechanisms and recent developments in different drug delivery vehicles, including the quantum dots, nano/micro particles, and molecular agents. Different loading strategies to incorporate the therapeutic reagents into the scaffolding structures are explored. Further, we discuss the main mechanisms to tune and monitor/quantify the release kinetics of embedded drugs from engineered scaffolds. We also survey the current trend of drug delivery using stimuli driven biopolymer scaffolds to enable precise spatiotemporal control of the release behavior. Recent advancements, challenges facing current scaffold-based drug delivery approaches, and areas of future research are discussed.

1. Introduction

Over the last few decades tissue engineering (TE) has evolved rapidly to address an ever-growing shortage of organ transplant donors, as well as establishing robust *in vitro* platforms to model a variety of biological processes in biomimetic microenvironments [1–3]. Among various TE approaches, porous scaffold systems, composed of various biomaterials, have emerged as an essential tool to facilitate the growth or repair of tissues and organs in both *in vitro* and *in vivo* applications [4]. In these biomaterial-based TE methods, the tissue-specific cells and/or support factors (e.g., growth or angiogenic factors) are loaded into a biocompatible scaffold with physiomechanical and biochemical properties that closely approximate those of the extracellular matrix (ECM) of the native tissue. These engineered devices provide a controlled microenvironment for endogenous and/or exogenous (transplanted) cell sources to migrate, grow, remodel the ECM, and function [5].

Concurrent with the rapid advancements in various fronts of TE, the field of drug delivery has also made great strides in biomedical applications, aiming to address the challenges faced in efficient and controlled delivery of therapeutics [6,7]. In principle, drug delivery systems focus on two specific forms of control: i) temporal control to deliver the proper dosage during a given time interval; and ii) spatial control to deliver the pharmaceutical agents to the precise site in the human body [8,9]. Over the last decades, various efforts have focused on designing new or enhanced biomaterial systems that exhibit controlled release of the selected therapeutics to ensure the efficacy of therapies. These materials can be accurately transplanted into the specific sites responsible for the disease state.

* Corresponding author at: 2015 Uppergate Dr., ECC Bldg., Suite E258, Atlanta, GA 30322, USA.
E-mail address: vahid.serpooshan@bme.gatech.edu (V. Serpooshan).

https://doi.org/10.1016/j.jconrel.2022.04.044
Received 21 February 2022; Received in revised form 24 April 2022; Accepted 27 April 2022
Available online 6 July 2022

Early drug delivery efforts utilized osmotic pumps, based on semi-permeable membrane or hydrophilic and hydrophobic polymers as an oral controlled release system [10]. Other drug delivery methods, such as drug eluting stents, have also demonstrated successful clinical applications [11]. Subsequent developments in material science allowed for creating delivery systems containing macromolecule drugs which can be controlled through diffusion within polymers [12]. Advancement in nanotechnology has expanded a new generation of functional smart materials, including biocompatible nanomaterials such as liposomes, dendrimers, polymer nanoparticles (NPs), and polymeric micelles [13–16].

Among various drug delivery vehicles, TE scaffold systems are advantageous due to several key characteristics, including: high porosity and surface area, excellent biocompatibility, controllable degradation, effective integration with the host tissue, and the ability for local and targeted delivery of therapeutics (Fig. 1) [17,18]. The local delivery of reagents at the tissue site can further enhance the efficacy of the drug and avoid the harmful off-target effects over the entire body [19,20]. The efficacy of 3D scaffold-based drug delivery systems has been investigated for different therapeutic applications such as bone [21], cartilage [22], and cardiovascular [23] tissues. This review aims to provide a comprehensive overview of the most recent developments in drug delivery processes, mediated via 3D scaffold devices, for diverse clinical applications. We will discuss the different drug loading and controlled release mechanisms, the main types of delivery agents used, and the strategies to monitor release from the TE structures. The goal is to inspire further research on using advanced biomaterials and bioengineering techniques to integrate TE and drug delivery approaches more effectively, hence offering enhanced scaffold-based therapies for clinical applications.

2. Design and fabrication of drug-loaded TE scaffolds

2.1. Strategies to incorporate therapeutics into 3D scaffolds

Several strategies have been developed to incorporate various drugs into the scaffolds for therapeutic applications, including direct loading, blending, and surface/chemical conjugation [24–26] (Fig. 2). These methods have important advantages and disadvantages with respect to the method of fabrication, the structure and desirable scaffold geometry, targeted therapeutics, controlled release, and specific clinical applications.

2.1.1. Direct loading

The direct loading technique employs the submersion of the scaffold in a therapeutic solution, which allows the drug molecules to attach to the scaffold surface via physical adsorption and/or absorption (Fig. 2A). For instance, scaffolds submerged in BMP-2 solution has been shown to be a viable method of promoting bone formation *in vivo* [27]. DeConde *et al.* demonstrated the effectiveness of biomimetic scaffolds impregnated with BMP-2 in regeneration of bone tissues in a marginal mandibular defect in rat model [28]. The delivery of exogenous growth factors, such as BMP-2, using an absorbable collagen sponge (ACS) has been promising and clinically successful for regenerating critical size bone defects. However, due to the poor affinity for the ACS, BMP-2 is rapidly released in a single, bolus dose. This requires the use of super-physiologic doses which in turn results in adverse outcomes and excessive treatment costs [29,30]. Another drawback of this method is that the loading capacity is strongly dependent on the morphology of the scaffolds such as the mesh size, scaffold free volume, the wettability matrix, and the physical characteristics of the therapeutics (e.g., molecular size) [31]. Nevertheless, submersion technique is widely used due to its simplicity and versatility since it can be integrated with a wide range of fabrication techniques.

2.1.2. Blended loading

In contrast to direct loading, blending technique involves the incorporation of the therapeutics into the scaffold materials before the formation of the 3D structure (Fig. 2B). This process is typically performed by mixing therapeutics with a polymer in a common solvent, which will be used to fabricate the 3D scaffold. An important advantage of this method is its compatibility with a variety of different scaffolding biomaterials, drugs, and synthesis techniques. For instance, electrospinning has been used to fabricate nanofiber scaffolds formed by a mixed solution of vitamin-B5 blended with PLCL/silk solutions for nerve tissue regeneration [32]. Murphy et al. developed a VEGF- encapsulated PLGA scaffolds by introducing the growth factors into a gas foaming/particulate leaching process [33]. Blending methods can be also applied to fabricate scaffolds via additive manufacturing technologies for applications that require complex structures. Shim et al. demonstrated the

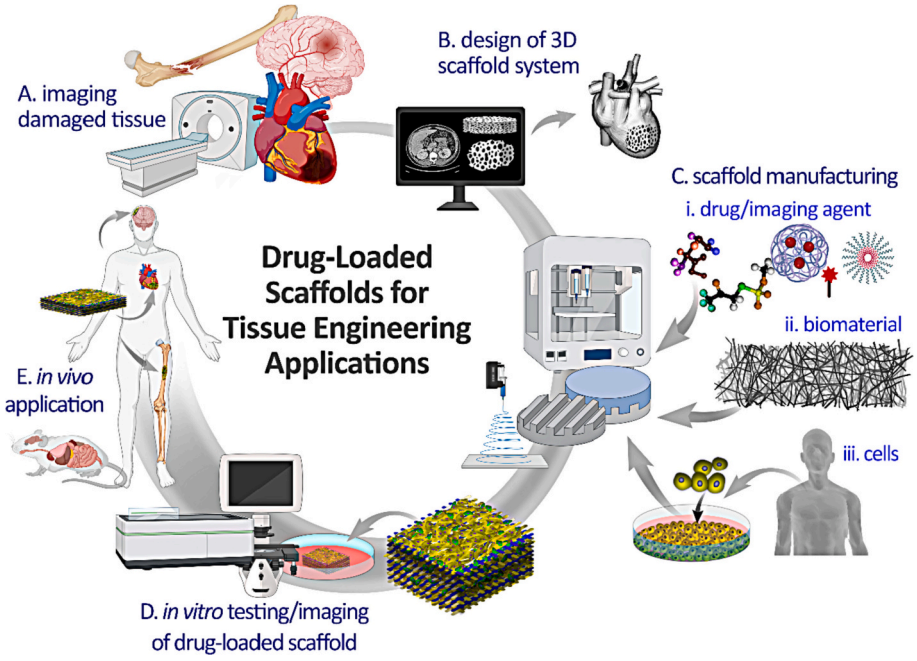

Fig. 1. Schematic illustration of the cycle to design, create, and utilize 3D functionalized scaffolds as drug delivery vehicles for tissue engineering applications. A-B: A variety of imaging techniques (A) can be used to create the digital CAD model of the scaffold (B). C: A drug-laden scaffold is fabricated using a combination of drug reagents, biomaterials, and cells, via various tissue manufacturing techniques, including 3D (bio)printing, electrospinning, and micropatterning. Therapeutics and/or labeling agents can be incorporated within the 3D scaffold through a variety of processes, including direct loading, blended loading, drug conjugation, and encapsulation techniques. D: *In vitro* characterization of drug-loaded scaffolds may include drug loading and stability, release kinetics, invasive and noninvasive imaging, and biological function, among others. E: Finally, optimized drug-laden scaffolds are utilized *in vivo*, as a drug delivery vehicle for sustained and targeted release of therapeutics to the site of injury.

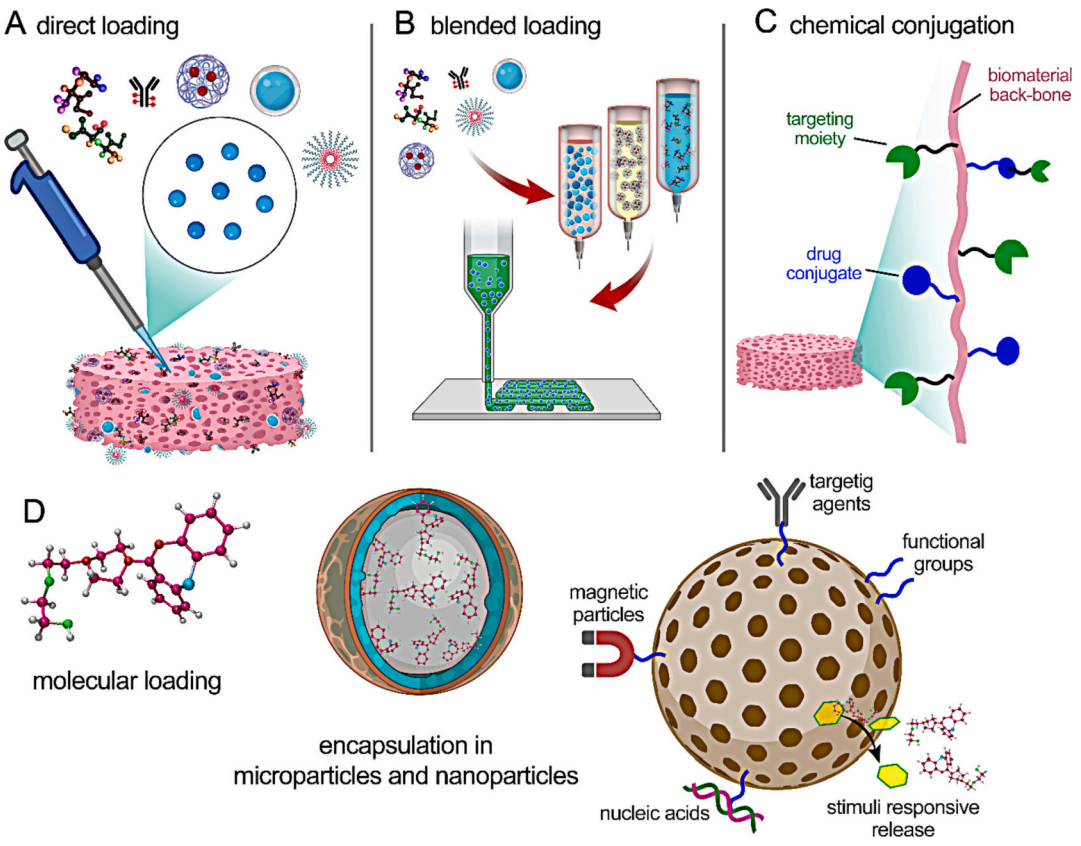

Fig. 2. Schematic illustration showing different mechanisms of loading therapeutics of various forms into tissue engineering scaffolds. A: Direct loading of drugs into a prefabricated scaffold and diffusion of reagents into the 3D porous structure. B: Blended loading: therapeutic reagents are mixed in the pre-polymerized biomaterial (e.g., bioink) and used to fabricate (e.g., 3D bioprint) the 3D scaffold structure. C: Chemical conjugation of therapeutic agents onto the biomaterial (polymer) molecule, which could be combined with addition of targeting moieties to enhance efficacy of delivery. D: Therapeutic reagents may be incorporated into the scaffold structures either directly (molecular loading, left), or via encapsulation in micro- and nanoparticles with different functionalities (middle and right).

controlled release of antibiotics (e.g. tobramycin) from a 3D printed scaffold using a filament consisting of polycaprolactone (PCL)/ poly lactic-co-glycolic acid (PLGA)/tobramycin blend [34]. However, one main limitation of loading therapeutics using blending is that the loading efficiency is highly dependent on the compatibility between the polymers and therapeutic molecules, which can result in inhomogeneous distribution of the therapeutic molecules and lower the overall loading capacity. In addition, this loading method offers little control over release kinetics. Kanematsu et al. investigated the release profiles in scaffolds fabricated by common aqueous solutions containing collagen type-I and different growth factors, such as basic fibroblast growth factor (bFGF), hepatocyte growth factor (HGF), platelet-derived growth factor (PDGF)-BB, vascular endothelial growth factor (VEGF), insulin-like growth factor (IGF)-1, and heparin-binding epidermal growth factor [35]. The study showed a burst effect and the drug release lasting for several days.

2.1.3. Chemical and surface conjugation

Chemical conjugation of drug molecules to scaffold materials or surfaces offers a means to overcome incompatibility between therapeutic molecules and the scaffold material, increase drug payload, and, most importantly, control release kinetics for sustained, triggered or on-demand drug release (Fig. 2C). For example, scaffold surfaces can be treated to induce certain chemical reactions, which are beneficial for drug binding. Most commonly, polymer surfaces are induced to form functional groups via aminolysis, hydrolysis, reduction, and oxidation [36]. These reactions can be facilitated by immersing polymer surfaces with NaOH, ethylenediamine, or N-aminoethyl-1,3-propanediamine to form carboxylic and amino groups [37,38]. The formation of these functional groups has been shown to enhance the loading of growth factors like BMP-2 in PCL scaffolds, while also moderating the burst effect and prolong the release time, when compared to untreated scaffolds [39].

In addition to surface treatment, chemical conjugation can also be applied to facilitate covalent linking to the scaffold material, thus immobilizing the therapeutics on the scaffold material or surface. Considering the robust binding of molecules, the chemical immobilization method is particularly suitable for slow and prolonged release of the therapeutic agents [40]. Typically, covalent-linking can be achieved through the reaction between the polymer functional groups and amine ligands found in proteins, or crosslinking agents [41]. In clinical applications like wound healing, the conjugation of growth factors like VGEF within a collagen matrix can enhance cell survival rate and promote angiogenesis [42]. However, these methods rely on the formation of certain chemical bonds on the scaffold surface. This limitation restricts the chemical composition of drugs available for loading. Furthermore, the immobilization process may not be suitable for drugs that are required to be endocytosed or to interact with the cell nuclei, unless significant scaffold degradation can mediate the effective drug release [40].

2.1.4. Loading bare drug molecules vs. encapsulation/loading in particle carriers

Therapeutic reagent could be loaded into the scaffolding systems either in their bare molecular form, or via encapsulation in (or conjugation on) a variety of micro- or nano-carriers (Fig. 2D). The latter approach has been particularly used to solve the incompatibility issues between scaffolds and therapeutics, via incorporating the biomolecular

agents into microparticles (MPs) or NPs before embedding within scaffolds. Loaded particles can be subsequently incorporated into the polymer networks pre- or post-fabrication of scaffolds, using direct loading, blended loading, or chemical conjugation strategies as outlined above (Fig. 2A-C).

2.1.4.1. Encapsulation in microparticles (MPs). Different biomaterials have been used for pre- or post-loading of pharmaceutical agents in the scaffold, ranging from MPs to nanostructures (Fig. 2D). Such encapsulations have been demonstrated, for instance, using polymeric MPs or NPs, or using PLGA microspheres or nanospheres. These strategies allow for better spatiotemporally control of multiple biological molecules [43], as well as programmed long-term sustained release of therapeutic factors [44,45]. Similarly, MPs have been also used to load NPs and other materials such as imaging contrast agents to improve localization for drug delivery. For use in protein therapy, PLGA (~10μm) and PEG-PLGA (~12 μm) MPs have been used as carriers for the growth factor neuregulin (NRG), as a potential treatment for myocardial infarction [46]. These particles have proven to allow the controlled release of NRG for at least 12 weeks in a murine model.

2.1.4.2. Encapsulation/loading in nanoparticles (NPs). Multifunctional NPs represent another pathway to incorporate a wide range of therapeutics into scaffolds. Yang *et al.* demonstrated the effectiveness of functionalized NPs, immobilized on scaffold surface with modified ligand, as carrier for genetic molecules such as DNA and siRNA to regulate cellular behavior [47]. Various types of NPs, such as quantum dots (QDs), silica, polystyrene, iron oxide, graphene, and lipid NPs, can offer the versatility in surface chemistry, thus allowing for precise control of conjugation with various ligands such as drugs, DNA, and targeting molecules [48–50], or with drug-loaded vesicles [51]. For example, Zhang *et al.* leveraged QD surface chemistry to synthesize QD-DNA hydrogels, functionalized with cancer targeting aptamers, to deliver siRNA and doxorubicin (DOX) as a cancer therapy [52]. Similarly, Fu et al. demonstrated the formation of QD-based drug delivery vehicles, tagged with redox-sensitive hyaluronic acid (HA) ligand, for targeted intracellular drug delivery to cancer cells [53]. The surface modification of QDs with multifunctional HA ligands offers a path to enhance loading and targeting efficiencies of the drug delivery systems.

2.2. Mechanisms of drug release in 3D scaffold systems

The design of 3D scaffolds is critically important in TE to mimic the physiomechanical and biochemical properties and functions of the native tissue ECM [54]. Ideally, the scaffolds need to provide a wide range of functions, including structural and physical cues for cellular growth and interactions, as well delivering different biological and pharmaceutical agents. The mechanism of drug delivery using porous scaffold systems can be controlled based on either passive or active transport of the drug molecules in the biomaterials comprising the scaffold architecture (Fig. 3) [55].

2.2.1. Diffusion

One strategy to facilitate the kinetics of drug release from 3D porous scaffolds is through the principle of molecular diffusion (Fig. 3). This physical phenomenon refers to the net transport of molecules from a region of higher concentration to one of lower concentration. Mathematically, certain assumptions can be adopted thus allowing for the prediction of the diffusion constant within the framework of Fick's first and second laws. For instance, to study the release process in a hydrogel-based scaffold, it is reasonable to assume a model where the therapeutic agents are surrounded by inert membranes, and diffusion rate is constant [56,57]. In the absence of leakage, the biomolecular concentration can be considered to be time-independent, and the concentration gradient throughout the membrane is constant, resulting in steady state

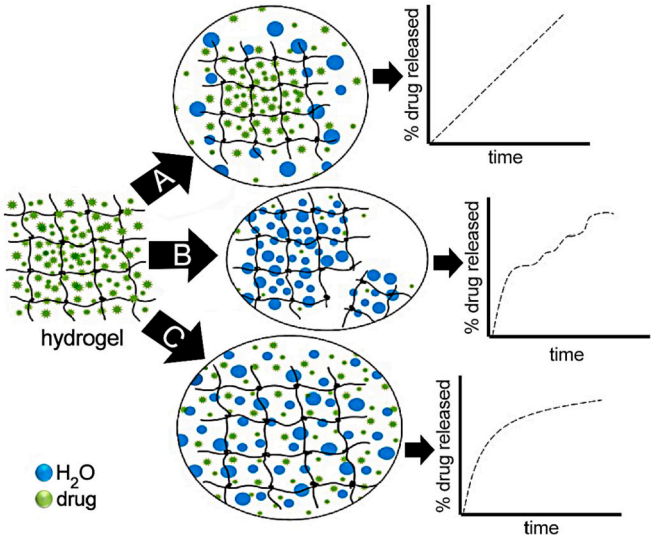

Fig. 3. Schematic design of different drug release mechanisms in 3D hydrogel scaffolds and the corresponding release kinetics. A: Molecular diffusion. B: Hydrogel matrix degradation. C: Hydrogel swelling. Reproduced with permission from Ref [55].

of release rate, which can be captured by Fick's first law as following

$$J = -D\nabla C$$

where D is the diffusion constant, J is the molecular flux of therapeutics, and ∇C is the concentration gradient. In a time-dependent release kinetics, Fick's second law can be adopted. For transport in one dimension, the equation of Fick's second law can be described as

$$\frac{dC}{dt} = D\frac{d^2C}{dx^2}$$

To optimally control the diffusion process of molecules in scaffolds, several physical parameters such as the size and chemistry of the hydrogel molecules and the environment temperature must be considered [58,59]. In many scaffolds, the free-volume of polymer can play a decisive role in controlling the diffusion rate, as higher free-volume allows for more water penetration inside the scaffold, thus enabling further drug diffusion and desorption. This effect has been observed by Pitt et al. when they compared the diffusion rate of therapeutics such as Quinine in scaffolds composed of different polymers (PCL and PLLA) [60]. In addition to free-volume, mesh size is also an important factor that can limit the specific sizes of the intended therapeutic molecules [56]. To overcome this challenge, mesh sizes can be tuned by modulating the concentration of polymers and crosslinking agents during scaffold formation [61].

2.2.2. Burst effect

Another important drug delivery mechanism is the burst release. This refers to the initial uncontrollable release of a large dose of therapeutics. Such an effect has been used as an optimal drug administering strategy for certain treatments like wound healing [62] where an initial rapid release can accelerate repair processes and relieve the patients' pain. However, burst release can also be harmful for patients in clinical applications. A number of factors have been attributed to causing the burst release, including the drug loading conditions and properties of hydrogels and drug molecules [57]. For instance, high-concentration drug loading can result in the drug molecules concentrating mostly on the scaffold surfaces, thus causing immediate release [63]. Vasudev et al. related the burst release of heparin to the different domain size in polyethylene vinyl acetate hydrogels [64]. The vesicles with high surface to volume ratio used to encapsulate drug molecules can also cause

the burst release. Specifically, MPs/NPs with large porosities can exhibit intense burst effect due to the fast diffusion of drugs through the large pores formed during synthesis conditions (Fig. 3) [65]. In addition, highly soluble drugs with small molecular weight are more prone to rapid diffusion through the hydrogel pores and causing the rapid release [66]. Understanding the actual mechanism of burst release is still an ongoing challenge since there is a lack of direct correlation between the *in vitro* versus *in vivo* release profiles, due to the complex interactions between therapeutic carriers and the *in vivo* environment [67,68].

To overcome the negative effect of burst release, several strategies have been devised to reduce/inhibit the burst release, including the use of crosslinkable polymeric coatings [69], increasing crosslinking density in the hydrogel [70], designing hybrid polymer blends [71], uneven loading of drug molecules with higher concentrations in the bulk scaffold [72], increasing the thickness of coating layer in molecular encapsulation [73], as well as engineering layer by layer scaffold structure with varying composition of drugs and polymers [74] (Fig. 4). Further, chemical and covalent conjugation, which were outlined in the previous section, are considered as another effective approach that can negate the burst release effect.

2.2.3. *Affinity-controlled release mechanism in TE scaffolds*

The drug release kinetics in scaffold can be controlled by modulating the physical and chemical interactions between drugs and the scaffolds. In passive drug delivery, the release kinetics is primarily mediated by the scaffold morphology, porosity, and structure, with minimal interactions between the drug and the scaffold. Further chemical and/or physical interactions between the scaffold host and the drug can be induced to offer more control over the release mechanism and kinetics. Chemically, this involves the degradation of the polymer chains mediated by hydrolysis [75] and enzyme activity [76]. Alternatively, certain complexes can be added to the polymer host, with strong affinity to the drug molecule(s), yielding a slower release profile. A major macromolecule family which has affinity to different drug molecules is β-cyclodextrins (CDs). Study by Mealy *et al.* showed the sustained release of a small molecule drug (L-tryptophan) over a 21-day time period in β-CD-modified hyaluronic acid (HA) hydrogel [77]. The release kinetics showed a sustainable slow-release profile with only ~ 20% of drug released within 24 hours compared to 90% release in untreated HA hydrogel. Consistent outcomes were observed by Lee *et al.*, examining the release of simvastatin attached to hydroxyapatite (HAp) NPs in β-CD coated PCL scaffold surface [78]. They reported an enhancement in drug loading as well as a slow-release profile up to 14 days, resulting in a greater growth and osteogenic differentiation *in vitro* and bone regeneration *in vivo* in comparison to untreated PCL scaffold. Another advancement in precise, spatio-temporally controlled drug release is to create ECM-mimetic scaffold microenvironment by decorating the matrix with molecules, such as heparin, and adhesive proteins with high affinity to biomolecules such as growth factors. Jha *et al.* studied the release process of transforming growth factor (TGF)-β1 in heparin-functionalized HA-based hydrogels [79]. The results demonstrated high drug loading capacity as well slow-release kinetics in the functionalized scaffold, which was primarily due to its higher affinity for TGFβ1. Further, Kisiel *et al.* reported the slow-release profile of BMP-2 delivered via fibronectin functionalized HA hydrogel [80].

The incorporation of functional NPs as a drug delivery vehicle/mechanism in the scaffold has been used as an alternative approach, allowing more freedom to control the release profile by modulating the NP-polymer matrix interactions. For instance, the drug release rate from hydrogels was suppressed after reinforcement with silicate NPs [81–83], likely due to NPs sterically inhibiting drug diffusion, reducing gel/scaffold swelling, and/or weakly binding to the drug via electrostatic interactions (Fig. 5A). As a drug carrier or delivery vehicle, the linkages between the drug and NP, or NP and scaffold, may be tailored to control release (Fig. 5B). Weak electrostatic or hydrolytically unstable linkages typically result in relatively rapid release. Therefore, strong covalent linkages have been used to enable sustained drug release. For example, iron oxide (Fe_3O_4) [84] and gold (Au) [85] NPs were covalently linked to collagen scaffolds such that release only occurred upon enzymatic degradation of the scaffold over several days.

2.2.4. *Stimuli driven control*

2.2.4.1. Release mechanism based on smart polymers. In addition to passive measure, active control of scaffolds composed of smart polymers has been implemented by exploiting their sensitivities to external factors, such as temperature, pH and natural stimuli like glucose for different therapeutic applications [86]. For instance, scaffold composed

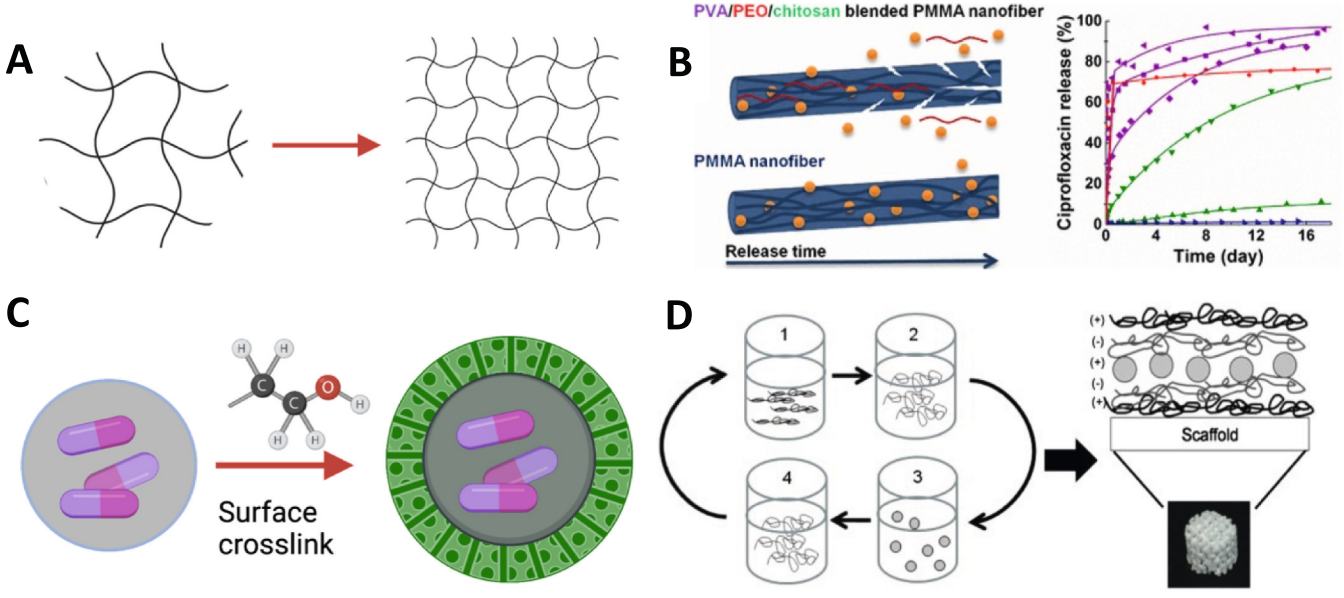

Fig. 4. Schematic illustration of different methods employed to mitigate burst release effect. A: Increasing crosslink density. B: Designing hybrid polymer blends. C: Creating functionalized coating through surface crosslinking. D: Layer-by-layer design and fabrication of the scaffold structure, laden with the therapeutic agents. Adapted with permission from [71,74].

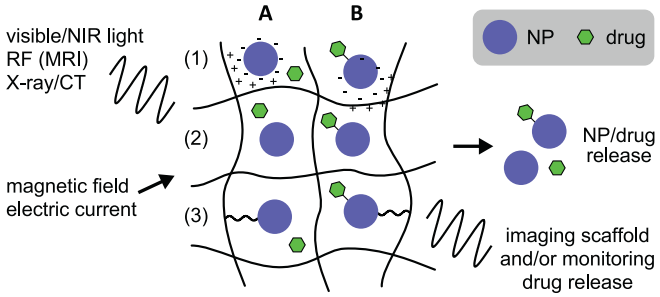

Fig. 5. Schematic diagram showing the incorporation of nanoparticles (NPs), either (A) alone or (B) as a drug carrier, in a scaffold by (1) electrostatic adsorption, (2) physical encapsulation or absorption, or (3) chemical conjugation. Importantly, NPs may act as a mechanical reinforcement, a bioactive agent, a drug carrier or delivery vehicle, a signal transducer for remotely triggering drug release, a contrast agent for imaging the scaffold by fluorescence, MRI and/or CT, and/or a diagnostic imaging probe for noninvasively monitoring drug release.

of thermosensitive polymers have been used to deliver pharmaceuticals such as docetaxel [87], exenatide [88], and leuprolide [89], for treatment of gastric cancer, type-II diabetes, and tumors, respectively. In these systems, the thermo-responsive polymers undergo a reversible sol-gel transition as the temperature increases which allows for precise control of rate of release of incorporated drugs, thus making them ideal for *in vivo* applications [90,91]. pH [92,93] and glucose [94] sensitive polymers can be used to deliver drugs like insulin or other pharmaceuticals that are sensitive to acid or base environments via the oral pathway. In addition to bioresponsive stimuli, external fields like electrical and magnetic fields [95,96], light [97], and ultrasound [98] have been used to induce mechanical stress on different hydrogels with active magnetic or piezoelectric properties to alter their topology, thus, facilitating the drug release process. Due to the versatility and tunability of the release mechanisms, smart hydrogel-based scaffolds play an increasingly important role in delivering different functional pharmaceuticals in clinical applications.

2.2.4.2. Release mechanism based on NP loading. As a signal transducer, NPs may be used to trigger drug release upon exposure to light, electrical current, and magnetic fields. The surface plasmon resonance of AuNPs was leveraged to enable light-activated switchable on/off drug release by photothermal heating of AuNPs incorporated within a thermally-sensitive hydrogel drug carrier [99–101]. Carbon nanotubes and graphene also exhibit a photothermal effect upon irradiation with near-infrared (NIR) light which has been used for light-activated drug release from thermally-sensitive hydrogels [102,103]. Doped lanthanide upconversion NPs were used to convert NIR light into UV light to disrupt the structure of the hydrogel and release encapsulated drugs on-demand [97]. The electrical conductivity of carbon nanotubes and graphene was also leveraged for controlled drug release from hydrogels upon electrical stimulation [104,105]. Finally, superparamagnetic iron oxide NPs (SPIONs) incorporated in hydrogels have been widely investigated for remotely triggering on/off drug release by opening/closing the pore network via NP aggregation/de-aggregation or heating/cooling upon switching a direct or alternating current magnetic field [106–109]. Moreover, a photocleavable drug-NP linkage enabled on-demand drug release from a hydrogel upon ultra-violet (UV) irradiation [110]. Overall, light-activated drug release offers the greatest temporal control, but activation and application are limited by the depth of light penetration in tissue and/or biomaterial. Activation by electric current exhibits lower temporal control and may require invasive electrical contacts. Magnetically activated drug release may offer the best balance of temporal control without a limit on the depth of tissue penetration.

In addition to acting as triggering mechanism to release conjugated therapeutics in the scaffold system, advancement in nanomaterial fabrication has created new "smart" nanocarriers that can have *dual function* as a drug carrier with on-demand release mechanism. For instance, nanochain structure comprised of magnetic nanospheres and doxorubicin-loaded liposome has displayed effective therapeutic behavior in tumor treatment [111]. Within these nanostructures, the magnetic NPs act as on-demand trigger mechanism to release the therapeutics incorporated in the liposome. As a result, they represent a new strategy to effectively control drug release for TE applications, provided that they can be effectively embedded within the scaffold matrix.

3. Noninvasive methods to monitor delivery and release of therapeutics from scaffolds

In addition to therapeutics, smart electronic materials, such as QDs [112], fluorescent sensitive semiconductors [113], or X-ray sensitive materials like gadolinium based molecular agents [114], can be also embedded within scaffolds, thus enabling the *in vivo* (or *in vitro*) tracking of the efficacy of drug delivery as well as the tissue/organ regeneration [115]. Typically, these materials can be incorporated in the scaffolds via a combination of surface conjugation, direct, and blended loading techniques depending on the surface functional groups of the polymer scaffolds and the molecular tracking agents, which also allows for the formation of scaffolds in various geometries. Consequently, an exciting prospect in the intersection between TE and drug delivery is the development of "organ-on-chip" platforms [116] which combine both therapeutics and diagnostics in a single platform, to rapidly decrease the cost of drug discovery process. A variety of imaging modalities have been adapted to monitor the drug-laden scaffold systems both *in vitro* and *in vivo* (**Table 1**).

3.1. Computed tomography (CT) techniques

CT is a noninvasive imaging technique with rapid acquisition time and high resolution, thus, allowing for more accurate monitoring of release kinetics [126]. A variety of CT molecular agents such as gadolinium and iodine contrast agents are commonly used in TE scaffolds to monitor and quantify the release behavior of therapeutics. Gadolinium is an FDA-approved contrast agent that is often used because it has a low detection limit, provides high relaxivity, and low toxicity for magnetic resonance imaging (MRI) [115,127–129]. Gadolinium can be used to quantify the integration and degradation of implanted hydrogel scaffolds in real time and without sacrificing samples [129,130]. Furthermore, gadolinium has shown potential in theranostic (therapeutic and diagnostic) applications via loading into core-shell fibers [131]. Using single photon emission CT (SPECT), iodine labeled BMP-2 pharmacokinetics and release profiles from bone tissue scaffolds were quantified [117,132]. The iodine-BMP conjugates have been imaged via micro-CT to monitor bone formation [117,132]. For cartilage tissue regeneration, cationic contrast agents (e.g., CA4+) are typically used because of their ability to increase X-ray signal attenuation [133–135]. This has been particularly useful in monitoring and quantifying changes in GAG content [133,135].

In addition to the molecular contrast agents, other compounds such as AuNPs [118,136] and a wide variety of other NP compositions containing high atomic number elements [137] can function effectively as contrast agent for X-ray CT [137,138]. For example, X-ray contrast of agarose and alginate scaffolds was enhanced by encapsulating Gd_2O_3, ZrO_2, Bi, and ZnO NPs. Gd_2O_3 NPs were used to noninvasively and longitudinally monitor the scaffold volume at high resolution after implantation [139]. AuNPs were covalently linked to collagen scaffolds to enable non-invasive, longitudinal, and volumetric X-ray imaging [85]. The scaffold degradation kinetics and AuNP release measured by CT during enzymatic degradation exhibited high precision as validated by chemical spectroscopy. In another study, incorporation of AuNPs into gelMA bioinks resulted in enhanced X-ray attenuation of 3D bioprinted

Table 1
Various imaging modalities used to monitor/quantify drug delivery and release in 3D scaffolds.

Imaging modality	Scaffold system	Therapeutic	Experimental conditions	Reference
Single photon emission CT	Polypropylene fumarate	BMP-2 labeled with iodine	Scaffold with therapeutics was implanted in a rat model	[117]
μCT	GelMA	Au nanoparticles (NPs)	Scaffold was 3D printed in a gelMA-Au bioink	[118]
μCT	GelMA and hyaluronic acid	Au NPs	Scaffold was 3D printed using methacrylate-modified gold nanoparticles covalently linked with methacrylate-modified hydrogels	[119]
MRI	Polyvinylidene fluoride (PVDF)	Superparamagnetic iron oxide NPs (SPIONs)	PVDF containing SPION encapsulation was implanted in human to treat hernia	[120]
MRI	Gelatin sponge (GS)	SPIONs	Scaffold containing SPIONs loaded gelatin sponge was implanted in the incisor sockets of Sprague-Dawley rats	[121]
MRI	Poly(propylene fumarate) (PPF)	Doxorubicin coated iron oxide (IONP) or manganese oxide nanoparticles (MONP)	Iron oxide NP or manganese oxide nanoparticles coated with doxorubicin were absorbed/mixed with the scaffold and their release kinetics was measured with MRI	[122]
Photoluminescence (PL)	Polyethylene Glycol (PEG)	Doxorubicin (DOX) with silver sulfide (Ag_2S) quantum dots (QDs)	DOX was loaded into PEG-coated Ag_2S QDs through hydrophobic-hydrophobic interactions	[123]
PL	PEG	Fluorescein-5-carboxyamido hexanoic acid	Fluorescein labelled PEG was implanted in mice model and the degradation of PEG hydrogel was monitored *in vivo* using PL technique	[124]
PL	Alginate hydrogel	Rhodamine	Modified alginate hydrogel seeded with MG-63 cells was developed by RGD peptide graft and gelatin microspheres labelled with rhodamine to monitor the degradation kinetics of microspheres	[125]

scaffolds. The functionalized scaffold system demonstrated adequate cell support and potential for use as implant for bone regenerative therapies [118] (Fig. 6). Further, AuMA NPs were recently used to prepare both conventional photopolymerized hydrogels and 3D bioprinted tissue scaffolds [119]. Fabricated scaffolds with tunable X-ray contrast enabled noninvasive, longitudinal monitoring of their placement, degradation, and NP release via micro-CT. It is noteworthy that several of the imaging efforts described here do not directly assess the drug delivery/release, instead, they monitor the degradation of the scaffolding systems and the resulting leakage of imaging probes.

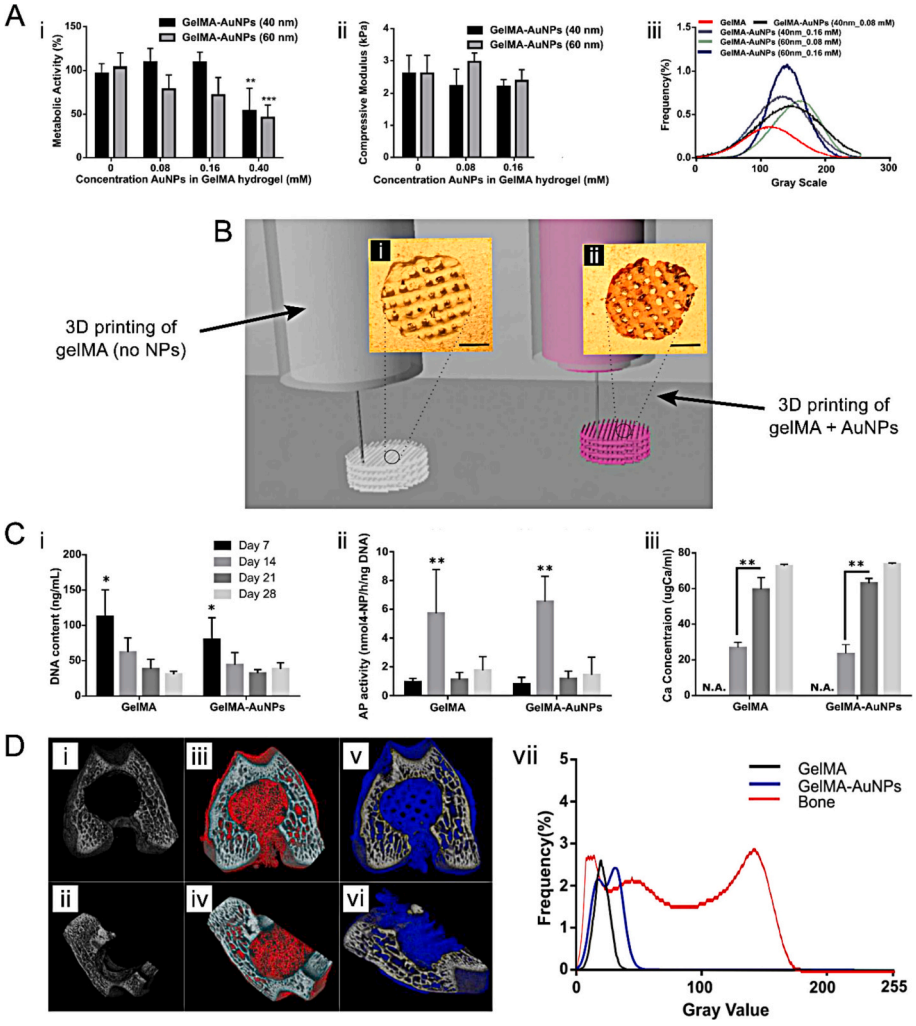

Fig. 6. Enhancing X-Ray attenuation of bioprinted gelatin methacrylate (gelMA) scaffolds using gold nanoparticles (AuNPs) for bone tissue engineering applications. A: Assessing *in vitro* biocompatibility (i), mechanical properties (ii), and μCT imaging properties (iii) of gelMA hydrogels containing varying levels of AuNPs at different sizes (pre-printing). B: The schematic illustration of 3D bioprinting gelMA (i) and gelMA-Au (ii) scaffolds. The insets show the color change in printed scaffolds as a result of AuNP incorporation in the bioink. C: Colorimetric quantification of DNA content in ng/mL (i), alkaline phosphatase (AP) activity (ii), and concentration of deposited calcium (Ca) (iii) after 28 days of *in vitro* culture of mesenchymal stem cells (MSCs) onto the gelMA and gelMA-AuNP scaffolds ($n = 5$ pe group). *: $p < 0.05$, **: $p < 0.01$. D: μCT images of the rat condyle defect in untreated state (i–ii) and after implantation of gelMA (iii–iv) and gelMA-AuNPs (v–vi) scaffolds along the transverse and coronal plane. vii: Measured radiopacity of gelMA and gelMA-AuNP hydrogels in comparison to the bone tissue. Adapted with permission from [118].

Utilizing molecular or NP based CT contrast agents, attached to therapeutics, to monitor their release, however, face several challenges. Certain chemical elements can have strong affinity with specific organs in the body, thus resulting in local tissue damage or toxicity due to the large local accumulation of the contrast agents at specific site in the body after detachment [140]. Specifically, iodine exhibits large affinity to the thyroid gland which can potentially lead to toxicity at large concentrations [117]. Thus, it is important that contrast agent concentration is carefully adjusted to accurately measure the release kinetics while reducing the cytotoxicity following the implantation *in vivo*.

3.2. Magnetic resonance imaging (MRI)

MRI has been an advantageous *in vivo* tracking method due to its minimal invasiveness and high temporal spatial resolution [115,141]. Although, slow acquisition times in MRI can result in tissue damage due to the long exposure time [126]. To further enhance the image resolution, a wide range of molecular systems, such as gadolinium, have been used as contrast agents. When incorporated in a PCL composite scaffold, gadolinium enhanced the contrast of MR image acquisition and allowed for real time imaging of bone regeneration [142]. The addition of gadolinium for enhancing MR images has also been used to quantify glycosaminoglycan (GAG) content in hydrogels, which is crucial for cartilage regeneration [143–145]. Gadolinium contrast agents used for MR imaging face, however, a major drawback as they tend to have chelate structure. Tight covalent grafting of gadolinium chelate to the hydrogel scaffold could result in large retention in the human body [146]. As a result, large concentration of gadolinium can lead to problems such as systematic fibrosis or retention in brain, thus, limiting their clinical application [147].

The most common NP contrast agents for MRI are SPION (Fe_3O_4) and Gd_2O_3 NPs, which provide strong (negative) T_2 and (positive) T_1 contrast, respectively [148]. SPIONs were encapsulated within polyvinylidene fluoride (PVDF) textiles to produce MRI-visible scaffolds [120,149,150] that are used clinically for hernia and pelvic floor repair. Noninvasive, longitudinal monitoring of scaffold degradation and/or drug release by MRI was enabled by SPIONs encapsulated within photocrosslinked polypropylene fumarate [122], gelatin [121] and cellulose/silk fibroin [151] scaffolds, or covalently linked to collagen scaffolds [84], which were released upon hydrolytic or enzymatic degradation, respectively (Fig. 7). Infection-resistant MR-visible scaffolds were also engineered by incorporation SPIONs into type I collagen gel scaffolds for both *in vitro* and *in vivo* monitoring of cardiac patch constructs [152]. Further, a new generation of damage-specific, hyperelastic bone scaffolds, loaded with SPIONs, were 3D bioprinted and used to repair large non-healing bone fractures in the rat model [153]. MR contrast agent NPs can be also used in conjunction with other therapeutics. For example, iron oxides-laden PLGA MPs (0.4 – 3μm) were synthesized as a potential for cell targeting therapies. Xu *et al.* demonstrated that cell internalization of the MPs did not compromise cell viability or phenotype while enhancing MR parameters to localize and measure the release [154].

3.3. Photoluminescence (PL)

Fluorescence detection is a non-invasive multichannel imaging technique that can be used to monitor drug release kinetics. This is typically accomplished using molecular drug-fluorophore conjugates, semiconducting quantum dots (QDs), or bioluminescent microRNAs. Specifically, common organic fluorescent molecules like fluorescein and rhodamine have been used widely to monitor the degradation of different hydrogel scaffolds like PEG [155] and alginate [125] hydrogel. In addition, fluorophores can be readily volume-loaded within silica NPs [156] or a silica shell on an NP core [157] to achieve a greater payload, solubility, and stability compared to surface conjugated fluorophores. Upconversion NPs have also enabled non-invasive fluorescence imaging of hydrogel scaffolds [102] and their degradation via NP release [158,159].

QDs are fluorescent semiconductor crystals on the nanoscale with unique optical properties due to their size and structure. QDs exhibit

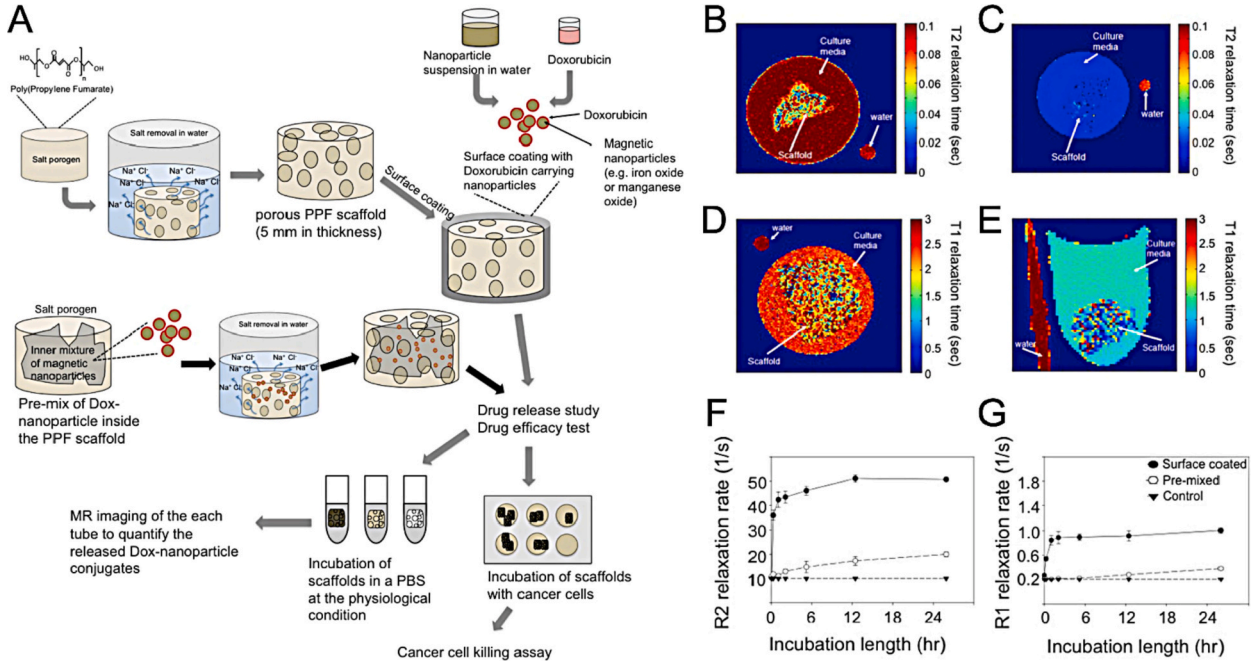

Fig. 7. Multimodal imaging of controlled drug release from 3D poly(propylene fumarate) (PPF) scaffolds. A: Schematic illustration of the biofabrication approach of PPF scaffolds and loading the drug-coated NPs. B: Quantitative analysis of drug release using MRI (T2 relaxation) signal of control (empty) scaffold (B), and PPF scaffolds coated with iron oxide NPs (IONPs) (C). D-E: MRI T1 relaxation map of control (D) and PPF scaffolds coated with manganese oxide NPs (MONPs) (E). All the MR data were acquired 48 hrs post incubation in PBS at 37°C. F-G: Plots of 1/T2 (F) and 1/T1 (G) relaxation *vs.* the incubation time for each scaffold group. Reproduced with permission from [122].

high photostability, brightness, size-tunability, and versatile surface chemistry that make them an attractive platform for studying drug delivery and release [160–163]. Most traditional fluorophores are highly susceptible to photobleaching which limit the intensity and duration of light exposure. In contrast, the superior photostability and brightness of QDs enable real-time imaging of drug delivery for long periods of time [123,164]. For example, Field *et al.* developed a multicomponent, QD-based drug system that can intracellularly release drug cargo upon addition of an extracellular trigger [165]. Here, QDs function as a Förster resonance energy-transfer (FRET) donor to attached dye/drug acceptor and increase photoluminescence (PL) upon drug conjugate release, therefore, facilitating real-time visualization of drug delivery into the cytoplasm. A major disadvantage which limits the applications of QDs is the potential cytotoxicity [161,166]. To overcome this challenge, QDs can be coated and passivated with shell or peptides and polymers to improve biocompatibility [165,167]. More recently, carbon-based QDs have been developed such as carbon QDs (CQDs) and graphene QDs (GQDs) that are biologically benign while maintaining superior photoelectric properties [168,169]. In addition, CQDs have been used in different therapeutic applications such as tissue engineering and cancer therapy [170]. For instance, sodium alginate-hemoglobin-CQDs hydrogel was applied to the bacterially infected wound area and the wound healing process was monitored under UV light conditions to monitor the changes in pH level (Fig. 8). The emission wavelength changed from green to blue after several days, due to the decreasing pH level because of the reduction of bacterial quantity through the Fenton, indicating that CQDs accelerated skin regeneration through better antibacterial activity.

For certain preclinical and clinical applications which require high biocompatibility, using fluorescently tagged microRNAs can provide a tool to study in real-time the effect of the microRNA on inducing vascular and bone regeneration [171]. Self-assembling peptides are amino acid sequences that form a variety of nanostructures and can deliver growth factors or drugs [172–174]. Release is regulated by tuning the peptide's sensitivity to pH, temperature, and light [172]. These peptides can be monitored and quantified via immunohistochemistry, fluorescent microscopy, and ELISA assay [173,174]. Lastly, the addition of luciferase and GFP to a collagen matrix has shown to be successful to perform longitudinal survival studies of implanted cardiomyoblast cell grafts [175]. These factors are biocompatible and can be monitored by fluorescent microscopy and immunohistochemistry, making them attractive additive to the TE scaffolds [175].

In summary, fluorescence imaging is indispensable in preclinical research, but has limited potential for clinical translation to humans due to the depth of light penetration being <1 cm even with NIR. Thus, NP probes for MRI and CT, which are not limited by tissue penetration, are critical for clinical translation. MRI offers greater sensitivity and does not expose the patient to ionizing radiation, but CT offers greater spatiotemporal resolution, lower cost, and wide availability. NP probes designed for multi-modal imaging can offer the benefits of both fluorescence and MRI or CT. It should be noted that in addition to imaging techniques reviewed here, several non-imaging techniques can be employed to assess and quantify drug release, such as sample and separate method (quantifying the supernatant, for *in vitro* release [176]) and blood test (for *in vivo* release [177,178]). These techniques, however, do not allow for *in-situ* monitoring of therapeutics release from the scaffolds and hence, are not the focus of this review.

4. Conclusions and future directions

In this review we outlined recent advancements in TE and drug delivery through several key progresses made in different areas of nano- and bio-technology, including smart biomaterials, bioactive drugs, and cell biology. These major advancements have resulted in the development of a new generation of functional scaffolds with increasingly precise spatiotemporal control of drug release to enhance the efficacy of tissue regeneration and cell signaling at the disease site. Moreover, the versatility in materials and architectures of scaffolds and therapeutic carriers has opened a new frontier of patient and damage/disease-specific regenerative therapies.

While significant progress has been made in different areas of scaffold-based drug delivery and noninvasive imaging of therapeutics in diverse TE applications, several challenges still hinder successful clinical translation. Considering the hydrophilic nature of hydrogels, the required hydration can provides practical challenges such as sterilization or storage condition for smart hydrogel scaffolds as drug delivery vehicles [179]. With respect to imaging of hydrogel structures via molecular agents, a number of technical challenges need to be addressed. An important challenge with the current contrast agents is that a critical, typically high concentration is required for imaging sequences.

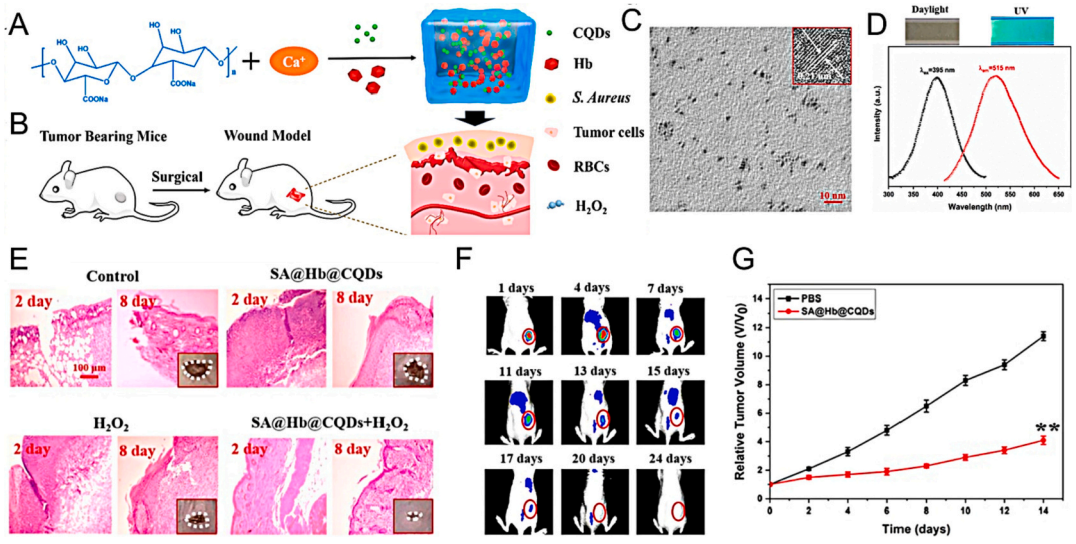

Fig. 8. Injectable self-crosslinking hydrogels consisting of hemoglobin (Hb), carbon quantum dots (CQDs), and sodium alginate (SA) for cancer therapy. A: Schematic illustration of synthesis of SA-Hb-CQDs. B: Establishment of postoperative tumor model and the corresponding status of wound. C: TEM images of CQDs. D: Photoluminescence (PL) spectra of CQDs. E: H&E images of the skin tissue samples of *S. aureus* infected wounds of mice after treating with samples at days 2 and 8. F: Dynamic fluorescence imaging of SA hydrogel containing indocyanine green-Hb-CQDs assembly in treated mice. G: Tumor volume change data. Reproduced with permission from [170].

Proposed strategy to overcome this problem is to use multiple relaxation agents, *e.g.*, EP-2104R containing 4 Gd-DOTA chelators [180], to overcome the problem of low efficacy of using just a single metal ion chelate bonded to the target vector. However, this method can itself face challenges with the synthesis. NP contrast agents have demonstrated great potential by enhancing the contrast due to their size and functionality, thus allowing for a large payload to be delivered to the target site [181,182]. A great concern for clinical translation is the toxicity at large concentration since the NPs cannot be entirely eliminated from the body [183,184].

In the case of NP-based drug delivery vehicles, another overlooked factor in the nano-bio interface is the formation of protein corona layer, i.e., the layer of biomolecules that forms on the surface of nanosized materials after their interactions with biological fluids. Protein corona on the surface of NPs can significantly alter the NP-cell interactions/uptake and, hence, the drug release profile of the nanocarriers [185,186]. Another challenge that may have important impact for clinical applications is the ability to control the release of different drugs using different delivery mechanisms with precise control throughout the lifetime of the system [187]. Biological sex also plays a significant role in the cell-(nano)biomaterials interactions and composition of protein corona, hence, causing substantial differences in the (nano)biomaterials' safety and efficacy in clinical applications [188–191]. A full consideration of the role of sex in the controlled release and drug delivery of nanocarriers enable researchers to design safer and more efficient nano-based drug delivery systems.

While these many challenges still exist, drug delivery in TE has begun to gain early adoption from the pharmaceutical industry. Different drug delivery encapsulated platforms have entered the market, most notably the Medtronic's INFUSE and MASTERGRAFT, as scaffold systems that can release BMP-2 drug for bone regeneration [187]. DEXTENZA developed by Ocular Therapeutix is another hydrogel system that can release dexamethasone after implantation for ocular treatments, which has just been recently approved by FDA [192]. The advent of new tissue biomanufacturing technologies, such as 3D bioprinting, has enabled fabrication of personalized and multi-functional TE scaffolds which would be of particular significance in the drug delivery and multi-contrast scaffold imaging applications [193]. Incorporation of multiple imaging contrast agents within engineered scaffolding system would be highly attractive, as it would enable simultaneous, longitudinal, and noninvasive monitoring of multiple functions of implanted scaffolds, such as the graft location/integration, blood perfusion, and drug release. With increasing understanding of how materials interact with tissue at a cellular level and advancements in disease-specific therapeutics like genetic nanomedicine, the new generation of scaffold-based delivery vehicles will not only overcome the shortcomings of conventional medicine but also establish a new paradigm of affordable and personalized medicine for the general public at a global scale.

Commercialization and translation of TE medical products would be greatly aided by the ability to non-invasively monitor the scaffold surgical placement, degradation and integration with the host tissue, and drug release, during both preclinical development and clinical applications. Such efforts would greatly decrease the burden (both financial and animal use) in preclinical regulatory testing phases.

Disclosures

The authors declare no conflicts of interest. Morteza Mahmoudi discloses that (i) he is a co-founder and director of the Academic Parity Movement (www.paritymovement.org), a non-profit organization dedicated to addressing academic discrimination, violence and incivility; (ii) he is a Founding Partner at Partners in Global Wound Care (PGWC); and (iii) he receives royalties/honoraria for his published books, plenary lectures, and licensed patent.

References

[1] R. Langer, J.P. Vacanti, Tissue engineering, Science 260 (1993) 920–926.
[2] A. Shafiee, A. Atala, Tissue engineering: toward a new era of medicine, Annu. Rev. Med. 68 (2017) 29–40.
[3] R. Langer, J. Vacanti, Advances in tissue engineering, J. Pediatr. Surg. 51 (2016) 8–12.
[4] K.Y. Lee, D.J. Mooney, Hydrogels for tissue engineering, Chem. Rev. 101 (2001) 1869–1879.
[5] M.P. Nikolova, M.S. Chavali, Recent advances in biomaterials for 3D scaffolds: a review, Bioact. Mater. 4 (2019) 271–292.
[6] K.R. Paudel, G.P. Rauniar, S.K. Bhattacharya, B.P. Das, Recent advancement in drug delivery system, Kathmandu Univ. Med. J. (KUMJ) 6 (2008) 262–267.
[7] Y.K. Sung, S.W. Kim, Recent advances in polymeric drug delivery systems, Biomater Res. 24 (2020) 12.
[8] N. Rahoui, B. Jiang, N. Taloub, Y.D. Huang, Spatio-temporal control strategy of drug delivery systems based nano structures, J. Control. Release 255 (2017) 176–201.
[9] M.L. Bruschi, 4 - Main mechanisms to control the drug release, in: M.L. Bruschi (Ed.), Strategies to Modify the Drug Release from Pharmaceutical Systems, Woodhead Publishing, 2015, pp. 37–62.
[10] R.A. Keraliya, C. Patel, P. Patel, V. Keraliya, T.G. Soni, R.C. Patel, M.M. Patel, Osmotic drug delivery system as a part of modified release dosage form, ISRN Pharm. 2012 (2012), 528079.
[11] T.F. Luscher, J. Steffel, F.R. Eberli, M. Joner, G. Nakazawa, F.C. Tanner, R. Virmani, Drug-eluting stent and coronary thrombosis: biological mechanisms and clinical implications, Circulation 115 (2007) 1051–1058.
[12] A. Kakkar, G. Traverso, O.C. Farokhzad, R. Weissleder, R. Langer, Evolution of macromolecular complexity in drug delivery systems, Nat. Rev. Chem. 1 (2017).
[13] O.C. Farokhzad, R. Langer, Impact of nanotechnology on drug delivery, ACS Nano 3 (2009) 16–20.
[14] M.J. Mitchell, M.M. Billingsley, R.M. Haley, M.E. Wechsler, N.A. Peppas, R. Langer, Engineering precision nanoparticles for drug delivery, Nat. Rev. Drug Discov. 20 (2021) 101–124.
[15] J.K. Patra, G. Das, L.F. Fraceto, E.V.R. Campos, M.D.P. Rodriguez-Torres, L. S. Acosta-Torres, L.A. Diaz-Torres, R. Grillo, M.K. Swamy, S. Sharma, S. Habtemariam, H.S. Shin, Nano based drug delivery systems: recent developments and future prospects, J. Nanobiotechnol. 16 (2018) 71.
[16] M.J. Hajipour, M. Mehrani, S.H. Abbasi, A. Amin, S.E. Kassaian, J.C. Garbern, G. Caracciolo, S. Zanganeh, M. Chitsazan, H. Aghaverdi, S.M. Kamali Shahri, A. Ashkarran, M. Raoufi, H. Bauser-Heaton, J. Zhang, J.D. Muehlschlegel, A. Moore, R.T. Lee, J.C. Wu, V. Serpooshan, M. Mahmoudi, Nanoscale technologies for prevention and treatment of heart failure: challenges and opportunities, Chem. Rev. 119 (2019) 11352–11390.
[17] T. Garg, O. Singh, S. Arora, R. Murthy, Scaffold: a novel carrier for cell and drug delivery, Crit. Rev. Ther. Drug Carrier Syst. 29 (2012) 1–63.
[18] R.A. Perez, H.-W. Kim, Core–shell designed scaffolds for drug delivery and tissue engineering, Acta Biomater. 21 (2015) 2–19.
[19] K.J. Rambhia, P.X. Ma, Controlled drug release for tissue engineering, J. Control. Release 219 (2015) 119–128.
[20] A.K. Ekenseair, F.K. Kasper, A.G. Mikos, Perspectives on the interface of drug delivery and tissue engineering, Adv. Drug Deliv. Rev. 65 (2013) 89–92.
[21] N. Subhapradha, M. Abudhahir, A. Aathira, N. Srinivasan, A. Moorthi, Polymer coated mesoporous ceramic for drug delivery in bone tissue engineering, Int. J. Biol. Macromol. 110 (2018) 65–73.
[22] S.L. Vega, M.Y. Kwon, J.A. Burdick, Recent advances in hydrogels for cartilage tissue engineering, Eur. Cell Mater 33 (2017) 59–75.
[23] H.S. O'Neill, L.B. Gallagher, J. O'Sullivan, W. Whyte, C. Curley, E. Dolan, A. Hameed, J. O'Dwyer, C. Payne, D. O'Reilly, E. Ruiz-Hernandez, E.T. Roche, F. J. O'Brien, S.A. Cryan, H. Kelly, B. Murphy, G.P. Duffy, Biomaterial-enhanced cell and drug delivery: lessons learned in the cardiac field and future perspectives, Adv. Mater. 28 (2016) 5648–5661.
[24] V. Mourino, A.R. Boccaccini, Bone tissue engineering therapeutics: controlled drug delivery in three-dimensional scaffolds, J. R. Soc. Interface 7 (2010) 209–227.
[25] T. Liang, J. Wu, F. Li, Z. Huang, Y. Pi, G. Miao, W. Ren, T. Liu, Q. Jiang, L. Guo, Drug-loading three-dimensional scaffolds based on hydroxyapatite-sodium alginate for bone regeneration, J. Biomed. Mater. Res. A 109 (2021) 219–231.
[26] M.L. Tomov, A. Theus, R. Sarasani, H. Chen, V. Serpooshan, 3D bioprinting of cardiovascular tissue constructs: cardiac bioinks, in: V. Serpooshan, S.M. Wu (Eds.), Cardiovascular Regenerative Medicine: Tissue Engineering and Clinical Applications, Springer International Publishing, Cham, 2019, pp. 63–77.
[27] K.H. Huang, Y.H. Lin, M.Y. Shie, C.P. Lin, Effects of bone morphogenic protein-2 loaded on the 3D-printed MesoCS scaffolds, J. Formos. Med. Assoc. 117 (2018) 879–887.
[28] A.S. DeConde, D. Sidell, M. Lee, O. Bezouglaia, K. Low, D. Elashoff, T. Grogan, S. Tetradis, T. Aghaloo, M. St John, Bone morphogenetic protein-2-impregnated biomimetic scaffolds successfully induce bone healing in a marginal mandibular defect, Laryngoscope 123 (2013) 1149–1155.
[29] W.F. McKay, S.M. Peckham, J.M. Badura, A comprehensive clinical review of recombinant human bone morphogenetic protein-2 (INFUSE® Bone Graft), Int. Orthop. 31 (2007) 729–734.
[30] M.G.L. Olthof, D.H.R. Kempen, X. Liu, M. Dadsetan, M.A. Tryfonidou, M. J. Yaszemski, W.J.A. Dhert, L. Lu, Bone morphogenetic protein-2 release profile modulates bone formation in phosphorylated hydrogel, J. Tissue Eng. Regen. Med. 12 (2018) 1339–1351.

[31] I.R. Calori, G. Braga, P.D.C.C. de Jesus, H. Bi, A.C. Tedesco, Polymer scaffolds as drug delivery systems, Eur. Polym. J. 129 (2020), 109621.
[32] M.A. Bhutto, T. Wu, B. Sun, H. Ei-Hamshary, S.S. Al-Deyab, X. Mo, Fabrication and characterization of vitamin B5 loaded poly (l-lactide-co-caprolactone)/silk fiber aligned electrospun nanofibers for schwann cell proliferation, Colloids Surf. B: Biointerfaces 144 (2016) 108–117.
[33] W.L. Murphy, M.C. Peters, D.H. Kohn, D.J. Mooney, Sustained release of vascular endothelial growth factor from mineralized poly(lactide-co-glycolide) scaffolds for tissue engineering, Biomaterials 21 (2000) 2521–2527.
[34] J.-H. Shim, M.-J. Kim, J.Y. Park, R.G. Pati, Y.-P. Yun, S.E. Kim, H.-R. Song, D.-W. Cho, Three-dimensional printing of antibiotics-loaded poly-ε-caprolactone/poly(lactic-co-glycolic acid) scaffolds for treatment of chronic osteomyelitis, Tissue Eng. Regenerat. Med. 12 (2015) 283–293.
[35] A. Kanematsu, S. Yamamoto, M. Ozeki, T. Noguchi, I. Kanatani, O. Ogawa, Y. Tabata, Collagenous matrices as release carriers of exogenous growth factors, Biomaterials 25 (2004) 4513–4520.
[36] S.K. Nemani, R.K. Annavarapu, B. Mohammadian, A. Raiyan, J. Heil, M.A. Haque, A. Abdelaal, H. Sojoudi, Surface Modification of Polymers: Methods and Applications 5, 2018, p. 1801247.
[37] T.I. Croll, A.J. O'Connor, G.W. Stevens, J.J. Cooper-White, Controllable surface modification of poly(lactic-co-glycolic acid) (PLGA) by hydrolysis or aminolysis I: physical, chemical, and theoretical aspects, Biomacromolecules 5 (2004) 463–473.
[38] Y. Cao, T.I. Croll, J.J. Cooper-White, A.J. O'Connor, G.W. Stevens, Production and surface modification of polylactide-based polymeric scaffolds for soft-tissue engineering, Methods Mol. Biol. 238 (2004) 87–112.
[39] L. Cao, Y. Yu, J. Wang, J.A. Werkmeister, K.M. McLean, C. Liu, 2-N, 6-O-sulfated chitosan-assisted BMP-2 immobilization of PCL scaffolds for enhanced osteoinduction, Mater. Sci. Eng. C Mater. Biol. Appl. 74 (2017) 298–306.
[40] M. Zamani, M.P. Prabhakaran, S. Ramakrishna, Advances in drug delivery via electrospun and electrosprayed nanomaterials, Int. J. Nanomedicine 8 (2013) 2997–3017.
[41] J.K. Tessmar, A.M. Gopferich, Matrices and scaffolds for protein delivery in tissue engineering, Adv. Drug Deliv. Rev. 59 (2007) 274–291.
[42] S. Koch, C. Yao, G. Grieb, P. Prevel, E.M. Noah, G.C. Steffens, Enhancing angiogenesis in collagen matrices by covalent incorporation of VEGF, J. Mater. Sci. Mater. Med. 17 (2006) 735–741.
[43] T.P. Richardson, M.C. Peters, A.B. Ennett, D.J. Mooney, Polymeric system for dual growth factor delivery, Nat. Biotechnol. 19 (2001) 1029–1034.
[44] R. Qodratnama, L.P. Serino, H.C. Cox, O. Qutachi, L.J. White, Formulations for modulation of protein release from large-size PLGA microparticles for tissue engineering, Mater. Sci. Eng. C Mater. Biol. Appl. 47 (2015) 230–236.
[45] J. Elisseeff, W. McIntosh, K. Fu, B.T. Blunk, R. Langer, Controlled-release of IGF-I and TGF-beta1 in a photopolymerizing hydrogel for cartilage tissue engineering, J. Orthop. Res. 19 (2001) 1098–1104.
[46] S. Pascual-Gil, T. Simon-Yarza, E. Garbayo, F. Prosper, M.J. Blanco-Prieto, Tracking the in vivo release of bioactive NRG from PLGA and PEG-PLGA microparticles in infarcted hearts, J. Control. Release 220 (2015) 388–396.
[47] F. Yang, S.W. Cho, S.M. Son, S.R. Bogatyrev, D. Singh, J.J. Green, Y. Mei, S. Park, S.H. Bhang, B.S. Kim, R. Langer, D.G. Anderson, Genetic engineering of human stem cells for enhanced angiogenesis using biodegradable polymeric nanoparticles, Proc. Natl. Acad. Sci. U. S. A. 107 (2010) 3317–3322.
[48] X.L. Cai, Y.N. Luo, W.Y. Zhang, D. Du, Y.H. Lin, pH-sensitive ZnO quantum dots-doxorubicin nanoparticles for lung cancer targeted drug delivery, ACS Appl. Mater. Interfaces 8 (2016) 22442–22450.
[49] R. Bilan, F. Fleury, I. Nabiey, A. Sukhanova, Quantum dot surface chemistry and functionalization for cell targeting and imaging, Bioconjug. Chem. 26 (2015) 609–624.
[50] T. Jamieson, R. Bakhshi, D. Petrova, R. Pocock, M. Imani, A.M. Seifalian, Biological applications of quantum dots, Biomaterials 28 (2007) 4717–4732.
[51] K.C. Weng, C.O. Noble, B. Papahadjopoulos-Sternberg, F.F. Chen, D. C. Drummond, D.B. Kirpotin, D.H. Wang, Y.K. Hom, B. Hann, J.W. Park, Targeted tumor cell internalization and imaging of multifunctional quantum dot-conjugated immunoliposomes in vitro and in vivo, Nano Lett. 8 (2008) 2851–2857.
[52] L.B. Zhang, S.R. Jean, S. Ahmed, P.M. Aldridge, X.Y. Li, F.J. Fan, E.H. Sargent, S. O. Kelley, Multifunctional quantum dot DNA hydrogels, Nat. Commun. 8 (2017) 9.
[53] Y. Fu, M.S. Jang, T.P. Wu, J.H. Lee, Y. Li, D.S. Lee, H.Y. Yang, Multifunctional hyaluronic acid-mediated quantum dots for targeted intracellular protein delivery and real-time fluorescence imaging, Carbohydr. Polym. 224 (2019) 9.
[54] F. Khan, M. Tanaka, Designing smart biomaterials for tissue engineering, Int. J. Mol. Sci. 19 (2017).
[55] D. Rocha-García, A. Guerra-Contreras, S. Rosales-Mendoza, G. Palestino, Role of porous silicon/hydrogel composites on drug delivery, Open Mat. Sci. 3 (2016).
[56] C.C. Lin, A.T. Metters, Hydrogels in controlled release formulations: network design and mathematical modeling, Adv. Drug Deliv. Rev. 58 (2006) 1379–1408.
[57] X. Huang, C.S. Brazel, On the importance and mechanisms of burst release in matrix-controlled drug delivery systems, J. Control. Release 73 (2001) 121–136.
[58] J. Siepmann, F. Siepmann, Modeling of diffusion controlled drug delivery, J. Control. Release 161 (2012) 351–362.
[59] C.S. Brazel, N.A. Peppas, Modeling of drug release from swellable polymers, Eur. J. Pharm. Biopharm. 49 (2000) 47–58.
[60] C.G. Pitt, A.R. Jeffcoat, R.A. Zweidinger, A. Schindler, Sustained drug delivery systems. I. The permeability of poly(epsilon-caprolactone), poly(DL-lactic acid), and their copolymers, J. Biomed. Mater. Res. 13 (1979) 497–507.
[61] F.J. Vernerey, E.C. Greenwald, S.J. Bryant, Triphasic mixture model of cell-mediated enzymatic degradation of hydrogels, Comput. Methods Biomech. Biomed. Eng. 15 (2012) 1197–1210.
[62] P. Heydari, A. Zargar Kharazi, S. Asgary, S. Parham, Comparing the wound healing effect of a controlled release wound dressing containing curcumin/ciprofloxacin and simvastatin/ciprofloxacin in a rat model: a preclinical study, J. Biomed. Mater. Res. A 110 (2022) 341–352.
[63] S.F. Chou, D. Carson, K.A. Woodrow, Current strategies for sustaining drug release from electrospun nanofibers, J. Control. Release 220 (2015) 584–591.
[64] S.C. Vasudev, T. Chandy, C.P. Sharma, Development of chitosan/polyethylene vinyl acetate co-matrix: controlled release of aspirin-heparin for preventing cardiovascular thrombosis, Biomaterials 18 (1997) 375–381.
[65] S. Kim, H. Sah, Merits of sponge-like PLGA microspheres as long-acting injectables of hydrophobic drug, J. Biomater. Sci. Polym. Ed. 30 (2019) 1725–1743.
[66] D.S. Hsieh, W.D. Rhine, R. Langer, Zero-order controlled-release polymer matrices for micro- and macromolecules, J. Pharm. Sci. 72 (1983) 17–22.
[67] Y. Fu, W.J. Kao, Drug release kinetics and transport mechanisms of non-degradable and degradable polymeric delivery systems, Exp. Opin Drug Deliv. 7 (2010) 429–444.
[68] M.E. Cam, S. Yildiz, H. Alenezi, S. Cesur, G.S. Ozcan, G. Erdemir, U. Edirisinghe, D. Akakin, D.S. Kuruca, L. Kabasakal, O. Gunduz, M. Edirisinghe, Evaluation of burst release and sustained release of pioglitazone-loaded fibrous mats on diabetic wound healing: an in vitro and in vivo comparison study, J. R. Soc. Interface 17 (2020) 20190712.
[69] M. Mahmoudi, A. Simchi, M. Imani, U.O. Häfeli, Superparamagnetic iron oxide nanoparticles with rigid cross-linked polyethylene glycol fumarate coating for application in imaging and drug delivery, J. Phys. Chem. C 113 (2009) 8124–8131.
[70] X. Huang, B.L. Chestang, C.S. Brazel, Minimization of initial burst in poly(vinyl alcohol) hydrogels by surface extraction and surface-preferential crosslinking, Int. J. Pharm. 248 (2002) 183–192.
[71] S. Zupancic, S. Sinha-Ray, S. Sinha-Ray, J. Kristl, A.L. Yarin, Long-term sustained ciprofloxacin release from PMMA and hydrophilic polymer blended nanofibers, Mol. Pharm. 13 (2016) 295–305.
[72] P.I. Lee, Effect of non-uniform initial drug concentration distribution on the kinetics of drug release from glassy hydrogel matrices, Polymer 25 (1984) 973–978.
[73] A.J. Thote, J.T. Chappell Jr., R.B. Gupta, R. Kumar, Reduction in the initial-burst release by surface crosslinking of PLGA microparticles containing hydrophilic or hydrophobic drugs, Drug Dev. Ind. Pharm. 31 (2005) 43–57.
[74] M.L. Macdonald, R.E. Samuel, N.J. Shah, R.F. Padera, Y.M. Beben, P. T. Hammond, Tissue integration of growth factor-eluting layer-by-layer polyelectrolyte multilayer coated implants, Biomaterials 32 (2011) 1446–1453.
[75] T.M. O'Shea, A.A. Aimetti, E. Kim, V. Yesilyurt, R. Langer, Synthesis and characterization of a library of in-situ curing, nonswelling ethoxylated polyol thiol-ene hydrogels for tailorable macromolecule delivery, Adv. Mater. 27 (2015) 65–72.
[76] M. Ishihara, K. Obara, T. Ishizuka, M. Fujita, M. Sato, K. Masuoka, Y. Saito, H. Yura, T. Matsui, H. Hattori, M. Kikuchi, A. Kurita, Controlled release of fibroblast growth factors and heparin from photocrosslinked chitosan hydrogels and subsequent effect on in vivo vascularization, J. Biomed. Mater. Res. A 64 (2003) 551–559.
[77] J.E. Mealy, C.B. Rodell, J.A. Burdick, Sustained small molecule delivery from injectable hyaluronic acid hydrogels through host-guest mediated retention, J. Mater. Chem. B 3 (2015) 8010–8019.
[78] J.B. Lee, J.E. Kim, M.S. Bae, S.A. Park, D.A. Balikov, H.J. Sung, H.B. Jeon, H. K. Park, S.H. Um, K.S. Lee, I.K. Kwon, Development of Poly(varepsilon-caprolactone) scaffold loaded with simvastatin and beta-cyclodextrin modified hydroxyapatite inclusion complex for bone tissue engineering, Polymers (Basel) 8 (2016).
[79] A.K. Jha, A. Mathur, F.L. Svedlund, J. Ye, Y. Yeghiazarians, K.E. Healy, Molecular weight and concentration of heparin in hyaluronic acid-based matrices modulates growth factor retention kinetics and stem cell fate, J. Control. Release 209 (2015) 308–316.
[80] M. Kisiel, M.M. Martino, M. Ventura, J.A. Hubbell, J. Hilborn, D.A. Ossipov, Improving the osteogenic potential of BMP-2 with hyaluronic acid hydrogel modified with integrin-specific fibronectin fragment, Biomaterials 34 (2013) 704–712.
[81] W.-F. Lee, Y.-T. Fu, Effect of montmorillonite on the swelling behavior and drug-release behavior of nanocomposite hydrogels 89, 2003, pp. 3652–3660.
[82] K.H. Liu, T.Y. Liu, S.Y. Chen, D.M. Liu, Drug release behavior of chitosan-montmorillonite nanocomposite hydrogels following electrostimulation, Acta Biomater. 4 (2008) 1038–1045.
[83] A.K. Mahanta, S. Senapati, P. Paliwal, S. Krishnamurthy, S. Hemalatha, P. Maiti, Nanoparticle-induced controlled drug delivery using chitosan-based hydrogel and scaffold: application to bone regeneration, Mol. Pharm. 16 (2019) 327–338.
[84] M.E. Mertens, A. Hermann, A. Buhren, L. Olde-Damink, D. Mockel, F. Gremse, J. Ehling, F. Kiessling, T. Lammers, Iron oxide-labeled collagen scaffolds for non-invasive MR imaging in tissue engineering, Adv. Funct. Mater. 24 (2014) 754–762.
[85] T.A. Finamore, T.E. Curtis, J.V. Tedesco, K. Grandfield, R.K. Roeder, Nondestructive, longitudinal measurement of collagen scaffold degradation using computed tomography and gold nanoparticles, Nanoscale 11 (2019) 4345–4354.
[86] H. Priya James, R. John, A. Alex, K.R. Anoop, Smart polymers for the controlled delivery of drugs - a concise overview, Acta Pharm. Sin. B 4 (2014) 120–127.

[87] W.K. Bae, M.S. Park, J.H. Lee, J.E. Hwang, H.J. Shim, S.H. Cho, D.E. Kim, H. M. Ko, C.S. Cho, I.K. Park, I.J. Chung, Docetaxel-loaded thermoresponsive conjugated linoleic acid-incorporated poloxamer hydrogel for the suppression of peritoneal metastasis of gastric cancer, Biomaterials 34 (2013) 1433–1441.

[88] K. Li, L. Yu, X. Liu, C. Chen, Q. Chen, J. Ding, A long-acting formulation of a polypeptide drug exenatide in treatment of diabetes using an injectable block copolymer hydrogel, Biomaterials 34 (2013) 2834–2842.

[89] M.H. Hsiao, M. Larsson, A. Larsson, H. Evenbratt, Y.Y. Chen, Y.Y. Chen, D.M. Liu, Design and characterization of a novel amphiphilic chitosan nanocapsule-based thermo-gelling biogel with sustained in vivo release of the hydrophilic anti-epilepsy drug ethosuximide, J. Control. Release 161 (2012) 942–948.

[90] Y. Qiu, K. Park, Environment-sensitive hydrogels for drug delivery, Adv. Drug Deliv. Rev. 53 (2001) 321–339.

[91] C. Gong, T. Qi, X. Wei, Y. Qu, Q. Wu, F. Luo, Z. Qian, Thermosensitive polymeric hydrogels as drug delivery systems, Curr. Med. Chem. 20 (2013) 79–94.

[92] K. Wang, X. Xu, Y. Wang, X. Yan, G. Guo, M. Huang, F. Luo, X. Zhao, Y. Wei, Z. Qian, Synthesis and characterization of poly(methoxyl ethylene glycol-caprolactone-co-methacrylic acid-co-poly(ethylene glycol) methyl ether methacrylate) pH-sensitive hydrogel for delivery of dexamethasone, Int. J. Pharm. 389 (2010) 130–138.

[93] S. Bazban-Shotorbani, M.M. Hasani-Sadrabadi, A. Karkhaneh, V. Serpooshan, K. I. Jacob, A. Moshaverinia, M. Mahmoudi, Revisiting structure-property relationship of pH-responsive polymers for drug delivery applications, J. Control. Release 253 (2017) 46–63.

[94] R. Yin, Z. Tong, D. Yang, J. Nie, Glucose and pH dual-responsive concanavalin A based microhydrogels for insulin delivery, Int. J. Biol. Macromol. 49 (2011) 1137–1142.

[95] X. Zhao, J. Kim, C.A. Cezar, N. Huebsch, K. Lee, K. Bouhadir, D.J. Mooney, Active scaffolds for on-demand drug and cell delivery, Proc. Natl. Acad. Sci. U. S. A. 108 (2011) 67–72.

[96] S. Murdan, Electro-responsive drug delivery from hydrogels, J. Control. Release 92 (2003) 1–17.

[97] B. Yan, J.C. Boyer, D. Habault, N.R. Branda, Y. Zhao, Near infrared light triggered release of biomacromolecules from hydrogels loaded with upconversion nanoparticles, J. Am. Chem. Soc. 134 (2012) 16558–16561.

[98] S. Mitragotri, Healing sound: the use of ultrasound in drug delivery and other therapeutic applications, Nat. Rev. Drug Discov. 4 (2005) 255–260.

[99] S.R. Sershen, S.L. Westcott, N.J. Halas, J.L. West, Temperature-sensitive polymer-nanoshell composites for photothermally modulated drug delivery, J. Biomed. Mater. Res. 51 (2000) 293–298.

[100] M. Bikram, A.M. Gobin, R.E. Whitmire, J.L. West, Temperature-sensitive hydrogels with SiO2-Au nanoshells for controlled drug delivery, J. Control. Release 123 (2007) 219–227.

[101] M. Amoli-Diva, R. Sadighi-Bonabi, K. Pourghazi, Switchable on/off drug release from gold nanoparticles-grafted dual light- and temperature-responsive hydrogel for controlled drug delivery, Mater. Sci. Eng. C Mater. Biol. Appl. 76 (2017) 242–248.

[102] Z. Cheng, R. Chai, P. Ma, Y. Dai, X. Kang, H. Lian, Z. Hou, C. Li, J. Lin, Multiwalled carbon nanotubes and NaYF4:Yb3+/Er3+ nanoparticle-doped bilayer hydrogel for concurrent NIR-triggered drug release and up-conversion luminescence tagging, Langmuir 29 (2013) 9573–9580.

[103] C.-H. Zhu, Y. Lu, J. Peng, J.-F. Chen, S.-H. Yu, Photothermally Sensitive Poly(N-isopropylacrylamide)/Graphene Oxide Nanocomposite Hydrogels as Remote Light-Controlled Liquid Microvalves 22, 2012, pp. 4017–4022.

[104] A. Servant, L. Methven, R.P. Williams, K. Kostarelos, Electroresponsive polymer-carbon nanotube hydrogel hybrids for pulsatile drug delivery in vivo, Adv. Healthc. Mater 2 (2013) 806–811.

[105] A. Servant, V. Leon, D. Jasim, L. Methven, P. Limousin, E.V. Fernandez-Pacheco, M. Prato, K. Kostarelos, Graphene-based electroresponsive scaffolds as polymeric implants for on-demand, Drug Deliv. 3 (2014) 1334–1343.

[106] T.Y. Liu, S.H. Hu, T.Y. Liu, D.M. Liu, S.Y. Chen, Magnetic-sensitive behavior of intelligent ferrogels for controlled release of drug, Langmuir 22 (2006) 5974–5978.

[107] Y. Zhang, T. Sun, C. Jiang, Biomacromolecules as carriers in drug delivery and tissue engineering, Acta Pharm. Sin. B 8 (2018) 34–50.

[108] T. Hoare, J. Santamaria, G.F. Goya, S. Irusta, D. Lin, S. Lau, R. Padera, R. Langer, D.S. Kohane, A Magnetically triggered composite membrane for on-demand drug delivery, Nano Lett. 9 (2009) 3651–3657.

[109] S. Merino, C. Martin, K. Kostarelos, M. Prato, E. Vazquez, Nanocomposite hydrogels: 3D polymer-nanoparticle synergies for on-demand drug delivery, ACS Nano 9 (2015) 4686–4697.

[110] S. Shah, P.K. Sasmal, K.B. Lee, Photo-triggerable hydrogel-nanoparticle hybrid scaffolds for remotely controlled drug delivery, J. Mater. Chem. B 2 (2014) 7685–7693.

[111] P.M. Peiris, L. Bauer, R. Toy, E. Tran, J. Pansky, E. Doolittle, E. Schmidt, E. Hayden, A. Mayer, R.A. Keri, M.A. Griswold, E. Karathanasis, Enhanced delivery of chemotherapy to tumors using a multicomponent nanochain with radio-frequency-tunable drug release, ACS Nano 6 (2012) 4157–4168.

[112] M.J. Molaei, Carbon quantum dots and their biomedical and therapeutic applications: a review, RSC Adv. 9 (2019) 6460–6481.

[113] W. Cui, X. Lu, K. Cui, J. Wu, Y. Wei, Q. Lu, Fluorescent nanoparticles of chitosan complex for real-time monitoring drug release, Langmuir 27 (2011) 8384–8390.

[114] N. Chawda, M. Basu, D. Majumdar, R. Poddar, S.K. Mahapatra, I. Banerjee, Engineering of gadolinium-decorated graphene oxide nanosheets for multimodal bioimaging and drug delivery, ACS Omega 4 (2019) 12470–12479.

[115] C.J. Gil, M.L. Tomov, A.S. Theus, A. Cetnar, M. Mahmoudi, V. Serpooshan, In Vivo Tracking of Tissue Engineered Constructs, Micromachines (Basel), 2019.

[116] D. Huh, B.D. Matthews, A. Mammoto, M. Montoya-Zavala, H.Y. Hsin, D.E. Ingber, Reconstituting organ-level lung functions on a chip, Science 328 (2010) 1662–1668.

[117] K. DH, Y. MJ, H. A, H. TE, C. LB, B. J, M. A, C. KL, D. WJ, L. L, Non-invasive Monitoring of BMP-2 Retention and Bone Formation in Composites for Bone Tissue Engineering Using SPECT/CT and Scintillation Probes, J. Control. Release 134 (2009).

[118] N. Celikkin, S. Mastrogiacomo, X.F. Walboomers, W. Swieszkowski, Enhancing X-ray attenuation of 3D printed gelatin methacrylate (GelMA) hydrogels utilizing gold nanoparticles for bone tissue engineering applications, Polymers (Basel) 11 (2019).

[119] L. Li, C.J. Gil, T.A. Finamore, C.J. Evans, M.L. Tomov, L. Ning, A. Theus, G. Kabboul, V. Serpooshan, R.K. Roeder, Methacrylate-modified gold nanoparticles enable noninvasive monitoring of photocrosslinked hydrogel scaffolds, Advanced NanoBiomed Research (2022), 2200022, https://doi.org/10.1002/anbr.202200022. In press.

[120] N.L. Hansen, A. Barabasch, M. Distelmaier, A. Ciritsis, N. Kuehnert, J. Otto, J. Conze, U. Klinge, R.D. Hilgers, C.K. Kuhl, N.A. Kraemer, First in-human magnetic resonance visualization of surgical mesh implants for inguinal hernia treatment, Investig. Radiol. 48 (2013) 770–778.

[121] S. Hu, Y. Zhou, Y. Zhao, Y. Xu, F. Zhang, N. Gu, J. Ma, M.A. Reynolds, Y. Xia, H.H. K. Xu, Enhanced bone regeneration and visual monitoring via superparamagnetic iron oxide nanoparticle scaffold in rats, J. Tissue Eng. Regen. Med. 12 (2018) e2085–e2098.

[122] J. Choi, K. Kim, T. Kim, G. Liu, A. Bar-Shir, T. Hyeon, M.T. McMahon, J.W. Bulte, J.P. Fisher, A.A. Gilad, Multimodal imaging of sustained drug release from 3-D poly(propylene fumarate) (PPF) scaffolds, J. Control. Release 156 (2011) 239–245.

[123] F. Hu, C. Li, Y. Zhang, M. Wang, D. Wu, Q. Wang, Real-time in vivo visualization of tumor therapy by a near-infrared-II Ag2S quantum dot-based theranostic nanoplatform, Nano Res. 8 (2015) 1637–1647.

[124] N. Artzi, N. Oliva, C. Puron, S. Shitreet, S. Artzi, A. bon Ramos, A. Groothuis, G. Sahagian, E.R. Edelman, In vivo and in vitro tracking of erosion in biodegradable materials using non-invasive fluorescence imaging, Nature Materials 10 (2011), 890-890.

[125] J. Sun, D. Wei, Y. Zhu, M. Zhong, Y. Zuo, H. Fan, X. Zhang, A spatial patternable macroporous hydrogel with cell-affinity domains to enhance cell spreading and differentiation, Biomaterials 35 (2014) 4759–4768.

[126] A. Szymanski-Exner, N.T. Stowe, K. Salem, R. Lazebnik, J.R. Haaga, D.L. Wilson, J. Gao, Noninvasive monitoring of local drug release using X-ray computed tomography: optimization and in vitro/in vivo validation, J. Pharm. Sci. 92 (2003) 289–296.

[127] M.S. Usman, M.Z. Hussein, S. Fakurazi, F.F. Ahmad Saad, Gadolinium-based layered double hydroxide and graphene oxide nano-carriers for magnetic resonance imaging and drug delivery, Chem. Cent. J. 11 (2017) 47.

[128] J. Tang, Y. Sheng, H. Hu, Y. Shen, Macromolecular MRI contrast agents: Structures, properties and applications | Elsevier Enhanced Reader, Prog. Polym. Sci. 38 (2013) 462–502.

[129] B.-V. D, D. W, H. A, O. D, H. J, Injectable Hyaluronic Acid Hydrogels With the Capacity for Magnetic Resonance Imaging, Carbohydrate polymers, 2018, p. 197.

[130] B. A, S.Y. H, D. H, N. M, S. D, Using bimodal MRI/fluorescence imaging to identify host angiogenic response to implants, in: Proceedings of the National Academy of Sciences of the United States of America, 2015, p. 112.

[131] J. M, Y. DG, G. CF, W. GR, B. SW, Theranostic fibers for simultaneous imaging and drug delivery, Mol. Pharm. 13 (2016).

[132] K. V, T. M, F. R, M. L, S. B, W. K, C. J, V.-N. G, K. DL, Porous silk fibroin 3-D scaffolds for delivery of bone morphogenetic protein-2 in vitro and in vivo, J. Biomed. Mater. Res. A 78 (2006).

[133] L. BA, P. H, H. C, F. JD, S. JS, S. BD, S. KS, G. MW, Contrast-enhanced CT using a cationic contrast agent enables non-destructive assessment of the biochemical and biomechanical properties of mouse tibial plateau cartilage, J. Orthop. Res. 34 (2016).

[134] S. de Bournonville, S. Vangrunderbeeck, G. Kerckhofs, Contrast-enhanced MicroCT for virtual 3D anatomical pathology of biological tissues: a literature review, Contrast Media Mol. Imag. 2019 (2019) 8617406.

[135] B. PN, J. NS, E. V, M. BC, S. RC, S. BD, G. MW, Cationic contrast agents improve quantification of glycosaminoglycan (GAG) content by contrast enhanced CT imaging of cartilage, J. Orthop. Res. 29 (2011).

[136] L.E. Cole, R.D. Ross, J.M. Tilley, T. Vargo-Gogola, R.K. Roeder, Gold nanoparticles as contrast agents in x-ray imaging and computed tomography 10 (2015) 321–341.

[137] P.F. FitzGerald, R.E. Colborn, P.M. Edic, J.W. Lambert, A.S. Torres, P. J. Bonitatibus Jr., B.M. Yeh, CT image contrast of high-Z elements: phantom imaging studies and clinical implications, Radiology 278 (2016) 723–733.

[138] M. Mahmoudi, V. Serpooshan, S. Laurent, Engineered nanoparticles for biomolecular imaging, Nanoscale 3 (2011) 3007–3026.

[139] S.M. Forton, M.T. Latourette, M. Parys, M. Kiupel, D. Shahriari, J.S. Sakamoto, E. M. Shapiro, In vivo microcomputed tomography of nanocrystal-doped tissue engineered scaffolds, ACS Biomater. Sci. Eng. 2 (2016) 508–516.

[140] J. Kim, P. Chhour, J. Hsu, H.I. Litt, V.A. Ferrari, R. Popovtzer, D.P. Cormode, Use of nanoparticle contrast agents for cell tracking with computed tomography, Bioconjug. Chem. 28 (2017) 1581–1597.

[141] B. Chertok, B.A. Moffat, A.E. David, F. Yu, C. Bergemann, B.D. Ross, V.C. Yang, Iron oxide nanoparticles as a drug delivery vehicle for MRI monitored magnetic targeting of brain tumors, Biomaterials 29 (2008) 487–496.
[142] N. Ganesh, A. Ashokan, R. Rajeshkannan, K. Chennazhi, M. Koyakutty, S.V. Nair, Magnetic resonance functional nano-hydroxyapatite incorporated poly (caprolactone) composite scaffolds for in situ monitoring of bone tissue regeneration by MRI, Tissue Eng. Part A 20 (2014) 2783–2794.
[143] A. AA, A. MA, L. JC, B. EM, Imaging challenges in biomaterials and tissue engineering, Biomaterials 34 (2013).
[144] R. S, U. MC, L. S, B. P, F. KW, S. RG, Noninvasive assessment of glycosaminoglycan production in injectable tissue-engineered cartilage constructs using magnetic resonance imaging, Tissue Eng. Part C Methods 14 (2008).
[145] N. AE, R. DA, F. KW, M. DL, M. T, B. D, R. S, S. RG, H. WE, Characterization of ex vivo-generated bovine and human cartilage by immunohistochemical, biochemical, and magnetic resonance imaging analyses, Tissue Eng. A 16 (2010).
[146] D. Bermejo-Velasco, W. Dou, A. Heerschap, D. Ossipov, J. Hilborn, Injectable hyaluronic acid hydrogels with the capacity for magnetic resonance imaging, Carbohydr. Polym. 197 (2018) 641–648.
[147] Y.C. Dong, M. Bouche, S. Uman, J.A. Burdick, D.P. Cormode, Detecting and monitoring hydrogels with medical imaging, ACS Biomater. Sci. Eng. 7 (2021) 4027–4047.
[148] H.B. Na, I.C. Song, T. Hyeon, Inorganic Nanoparticles for MRI Contrast Agents 21, 2009, pp. 2133–2148.
[149] N.A. Kramer, H.C. Donker, J. Otto, M. Hodenius, J. Senegas, I. Slabu, U. Klinge, M. Baumann, A. Mullen, B. Obolenski, R.W. Gunther, G.A. Krombach, A concept for magnetic resonance visualization of surgical textile implants, Investig. Radiol. 45 (2010) 477–483.
[150] M.E. Mertens, S. Koch, P. Schuster, J. Wehner, Z. Wu, F. Gremse, V. Schulz, L. Rongen, F. Wolf, J. Frese, V.N. Gesche, M. van Zandvoort, P. Mela, S. Jockenhoevel, F. Kiessling, T. Lammers, USPIO-labeled textile materials for non-invasive MR imaging of tissue-engineered vascular grafts, Biomaterials 39 (2015) 155–163.
[151] Z. Chen, C. Yan, S. Yan, Q. Liu, M. Hou, Y. Xu, R. Guo, Non-invasive monitoring of in vivo hydrogel degradation and cartilage regeneration by multiparametric MR imaging, Theranostics 8 (2018) 1146–1158.
[152] M. Mahmoudi, M. Zhao, Y. Matsuura, S. Laurent, P.C. Yang, D. Bernstein, P. Ruiz-Lozano, V. Serpooshan, Infection-resistant MRI-visible scaffolds for tissue engineering applications, Bioimpacts 6 (2016) 111–115.
[153] M. Shokouhimehr, A.S. Theus, A. Kamalakar, L. Ning, C. Cao, M.L. Tomov, J. M. Kaiser, S. Goudy, N.J. Willett, H.W. Jang, C.N. LaRock, P. Hanna, A. Lechtig, M. Yousef, J.D.S. Martins, A. Nazarian, M.B. Harris, M. Mahmoudi, V. Serpooshan, 3D bioprinted bacteriostatic hyperelastic bone scaffold for damage-specific bone regeneration, Polymers (Basel) 13 (2021).
[154] C. Xu, D. Miranda-Nieves, J.A. Ankrum, M.E. Matthiesen, J.A. Phillips, I. Roes, G. R. Wojtkiewicz, V. Juneja, J.R. Kultima, W. Zhao, P.K. Vemula, C.P. Lin, M. Nahrendorf, J.M. Karp, Tracking mesenchymal stem cells with iron oxide nanoparticle loaded Poly(lactide-co-glycolide) microparticles, Nano Lett. 12 (2012) 4131–4139.
[155] Y. Zhang, J. Yang, Design strategies for fluorescent biodegradable polymeric biomaterials, J. Mater. Chem. B Mater. Biol. Med. 1 (2) (2013) 132.
[156] W. Wang, P.D. Nallathamby, C.M. Foster, J.L. Morrell-Falvey, N.P. Mortensen, M. J. Doktycz, B. Gu, S.T. Retterer, Volume labeling with Alexa Fluor dyes and surface functionalization of highly sensitive fluorescent silica (SiO2) nanoparticles, Nanoscale 5 (2013) 10369–10375.
[157] P.D. Nallathamby, J. Hopf, L.E. Irimata, T.L. McGinnity, R.K. Roeder, Preparation of fluorescent Au-SiO2 core-shell nanoparticles and nanorods with tunable silica shell thickness and surface modification for immunotargeting, J. Mater. Chem. B 4 (2016) 5418–5428.
[158] G. Jalani, R. Naccache, D.H. Rosenzweig, S. Lerouge, L. Haglund, F. Vetrone, M. Cerruti, Real-time, non-invasive monitoring of hydrogel degradation using LiYF4:Yb3+/Tm3+ NIR-to-NIR upconverting nanoparticles, Nanoscale 7 (2015) 11255–11262.
[159] Y. Dong, G. Jin, C. Ji, R. He, M. Lin, X. Zhao, A. Li, T.J. Lu, F. Xu, Non-invasive tracking of hydrogel degradation using upconversion nanoparticles, Acta Biomater. 55 (2017) 410–419.
[160] C.E. Probst, P. Zrazhevskiy, V. Bagalkot, X.H. Gao, Quantum dots as a platform for nanoparticle drug delivery vehicle design, Adv. Drug Deliv. Rev. 65 (2013) 703–718.
[161] R. Bilan, I. Nabiev, A. Sukhanova, Quantum dot-based nanotools for bioimaging, diagnostics, and drug delivery, ChemBioChem 17 (2016) 2103–2114.
[162] C.T. Matea, T. Mocan, F. Tabaran, T. Pop, O. Mosteanu, C. Puia, C. Iancu, L. Mocan, Quantum dots in imaging, drug delivery and sensor applications, Int. J. Nanomedicine 12 (2017) 5421–5431.
[163] A.M. Smith, H.W. Duan, A.M. Mohs, S.M. Nie, Bioconjugated quantum dots for in vivo molecular and cellular imaging, Adv. Drug Deliv. Rev. 60 (2008) 1226–1240.
[164] I.B. Bwatanglang, F. Mohammad, N.A. Yusof, J. Abdullah, M.Z. Hussein, N. B. Alitheen, N. Abu, Folic acid targeted Mn:ZnS quantum dots for theranostic applications of cancer cell imaging and therapy, Int. J. Nanomedicine 11 (2016) 413–428.
[165] L.D. Field, S.A. Walper, K. Susumu, G. Lasarte-Aragones, E. Oh, I.L. Medintz, J. B. Delehanty, A quantum dot-protein bioconjugate that provides for extracellular control of intracellular drug release, Bioconjug. Chem. 29 (2018) 2455–2467.
[166] R. Hardman, A toxicologic review of quantum dots: toxicity depends on physicochemical and environmental factors, Environ. Health Perspect. 114 (2006) 165–172.
[167] M.J.D. Clift, J. Varet, S.M. Hankin, B. Brownlee, A.M. Davidson, C. Brandenberger, B. Rothen-Rutishauser, D.M. Brown, V. Stone, Quantum dot cytotoxicity in vitro: an investigation into the cytotoxic effects of a series of different surface chemistries and their core/shell materials, Nanotoxicology 5 (2011) 664–674.
[168] H. Ding, F. Zhang, C.C. Zhao, Y.L. Lv, G.H. Ma, W. Wei, Z.Y. Tian, Beyond a carrier: graphene quantum dots as a probe for programmatically monitoring anti-cancer drug delivery, release, and response, ACS Appl. Mater. Interfaces 9 (2017) 27396–27401.
[169] R. Jelinek, Carbon quantum dots: synthesis, properties and applications, carbon quantum dots: synthesis, Propert. Applic. (2017) 1–130.
[170] Q. Zhang, Z. Li, M. Zhang, W. Wang, J. Shen, Z. Ye, N. Zhou, Injectable in situ self-cross-linking hydrogels based on hemoglobin, carbon quantum dots, and sodium alginate for real-time detection of wound bacterial infection and efficient postoperative prevention of tumor recurrence, Langmuir 36 (2020) 13263–13273.
[171] L. Y, F. L, L. S, L. W, Z. H, Z. T, W. D, Y. P, S. L, C. J, J. Y, The promotion of bone regeneration through positive regulation of angiogenic-osteogenic coupling using microRNA-26a, Biomaterials 34 (2013).
[172] O.F. Khan, E. Cusano, S. Raissouni, M. Pabia, J. Haeseker, N. Bosma, J.J. Ko, H. Li, A. Kumar, M.M. Vickers, P.A. Tang, Immediate-term cognitive impairment following intravenous (IV) chemotherapy: a prospective pre-post design study, BMC Cancer 19 (2019) 150.
[173] H. PC, D. ME, G. J, M. C, L. RT, Controlled delivery of PDGF-BB for myocardial protection using injectable self-assembling peptide nanofibers, J. Clin. Invest. (2006) 116.
[174] S. K, F. T, Y. A, M. S, T. S, A. N, O. T, Combined use of bFGF and GDF-5 enhances the healing of medial collateral ligament injury, Biochem. Biophys. Res. Commun. 402 (2010).
[175] K. I, C. IY, K. T, V.D. G, S. AY, H. SL, H. G, P. J, B. HM, G. SS, R. RC, In Vivo Optical Bioluminescence Imaging of Collagen-Supported Cardiac Cell Grafts, J. Heart Lung Transplant. 26 (2007).
[176] Y. Kim, E.J. Park, T.W. Kim, D.H. Na, Recent progress in drug release testing methods of biopolymeric particulate system, Pharmaceutics 13 (2021).
[177] G.A. Reed, Stability of drugs, drug candidates, and metabolites in blood and plasma, Curr. Protoc. Pharmacol. 75 (2016) 7.6.1–7.6.12.
[178] V. Serpooshan, S. Sivanesan, X. Huang, M. Mahmoudi, A.V. Malkovskiy, M. Zhao, M. Inayathullah, D. Wagh, X.J. Zhang, S. Metzler, D. Bernstein, J.C. Wu, P. Ruiz-Lozano, J. Rajadas, [Pyr1]-Apelin-13 delivery via nano-liposomal encapsulation attenuates pressure overload-induced cardiac dysfunction, Biomaterials 37 (2015) 289–298.
[179] A. Wurm, M. Nogler, C.G. Ammann, D.C. Coraca-Huber, Effect of storage temperature and antibiotic impregnation on the quantity of bone morphogenetic protein seven in human bone grafts, Int. Orthop. 38 (2014) 1513–1517.
[180] J. Vymazal, E. Spuentrup, G. Cardenas-Molina, A.J. Wiethoff, M.G. Hartmann, P. Caravan, E.C. Parsons Jr., Thrombus imaging with fibrin-specific gadolinium-based MR contrast agent EP-2104R: results of a phase II clinical study of feasibility, Investig. Radiol. 44 (2009) 697–704.
[181] S.M. Janib, A.S. Moses, J.A. MacKay, Imaging and drug delivery using theranostic nanoparticles, Adv. Drug Deliv. Rev. 62 (2010) 1052–1063.
[182] C. Sun, J.S.H. Lee, M. Zhang, Magnetic nanoparticles in MR imaging and drug delivery, Adv. Drug Deliv. Rev. 60 (2008) 1252–1265.
[183] J. Wahsner, E.M. Gale, A. Rodriguez-Rodriguez, P. Caravan, Chemistry of MRI contrast agents: current challenges and new frontiers, Chem. Rev. 119 (2019) 957–1057.
[184] A.A. Saei, M. Yazdani, S.E. Lohse, Z. Bakhtiary, V. Serpooshan, M. Ghavami, M. Asadian, S. Mashaghi, E.C. Dreaden, A. Mashaghi, M. Mahmoudi, Nanoparticle surface functionality dictates cellular and systemic toxicity, Chem. Mater. 29 (2017) 6578–6595.
[185] S. Behzadi, V. Serpooshan, R. Sakhtianchi, B. Muller, K. Landfester, D. Crespy, M. Mahmoudi, Protein corona change the drug release profile of nanocarriers: the "overlooked" factor at the nanobio interface, Colloids Surf. B: Biointerfaces 123 (2014) 143–149.
[186] S. Sharifi, G. Caracciolo, M. Mahmoudi, Biomolecular corona affects controlled release of drug payloads from nanocarriers, Trends Pharmacol. Sci. 41 (2020) 641–652.
[187] J. Li, D.J. Mooney, Designing hydrogels for controlled drug delivery, Nat. Rev. Mater 1 (2016).
[188] S. Sharifi, G. Caracciolo, D. Pozzi, L. Digiacomo, J. Swann, H.E. Daldrup-Link, M. Mahmoudi, The role of sex as a biological variable in the efficacy and toxicity of therapeutic nanomedicine, Adv. Drug Deliv. Rev. 174 (2021) 337–347.
[189] C.M. Madla, F.K.H. Gavins, H.A. Merchant, M. Orlu, S. Murdan, A.W. Basit, Let's talk about sex: differences in drug therapy in males and females, Adv. Drug Deliv. Rev. 175 (2021), 113804.
[190] J.-L.J. Yang, R. Narayanamurthy, J.Y. Yager, L.D. Unsworth, How does biological sex affect the physiological response to nanomaterials? Nano Today 41 (2021), 101292.
[191] M.J. Hajipour, H. Aghaverdi, V. Serpooshan, H. Vali, S. Sheibani, M. Mahmoudi, Sex as an important factor in nanomedicine, Nat. Commun. 12 (2021) 2984.
[192] R. Narayanaswamy, V.P. Torchilin, Hydrogels and their applications in targeted drug delivery, Molecules 24 (2019).
[193] C. Gil, C. Evans, L. Li, M. Vargas, G. Kabboul, T. Fulton, R. Veneziano, N. Nick, H. Bauser-Heaton, R.K. Roeder, V. Serpooshan, Abstract MP207: a precision medicine approach for non-invasive, longitudinal, and quantitative monitoring of cardiac tissue-engineered scaffolds, Circ. Res. 129 (2021). AMP207-AMP207.